CrossMark
click for updates

The Glycolytic Enzyme Triosephosphate Isomerase of *Trichomonas vaginalis* Is a Surface-Associated Protein Induced by Glucose That Functions as a Laminin- and Fibronectin-Binding Protein

Jesús F. T. Miranda-Ozuna,[a] Mar S. Hernández-García,[a] Luis G. Brieba,[b] Claudia G. Benítez-Cardoza,[c] Jaime Ortega-López,[d] Arturo González-Robles,[a] Rossana Arroyo[a]

Departamento de Infectómica y Patogénesis Molecular, Centro de Investigación y de Estudios Avanzados del Instituto Politécnico Nacional (CINVESTAV-IPN), Mexico City, Mexico[a]; Laboratorio Nacional de Genómica para la Biodiversidad, CINVESTAV-IPN, Irapuato, Guanajuato, Mexico[b]; Laboratorio de Investigación Bioquímica, Programa Institucional en Biomedicina Molecular, ENMyH-IPN, Mexico City, Mexico[c]; Departamento de Biotecnología y Bioingeniería, CINVESTAV-IPN, Mexico City, Mexico[d]

Triosephosphate isomerase of *Trichomonas vaginalis* (*Tv*TIM) is a 27-kDa cytoplasmic protein encoded by two genes, *tvtim1* and *tvtim2*, that participates in glucose metabolism. *Tv*TIM is also localized to the parasite surface. Thus, the goal of this study was to identify the novel functions of the surface-associated *Tv*TIM in *T. vaginalis* and to assess the effect of glucose as an environmental factor that regulates its expression and localization. Reverse transcription-PCR (RT-PCR) showed that the *tvtim* genes were differentially expressed in response to glucose concentration. *tvtim1* was overexpressed under glucose-restricted (GR) conditions, whereas *tvtim2* was overexpressed under glucose-rich, or high-glucose (HG), conditions. Western blot and indirect immunofluorescence assays also showed that glucose positively affected the amount and surface localization of *Tv*TIM in *T. vaginalis*. Affinity ligand assays demonstrated that the recombinant *Tv*TIM1 and *Tv*TIM2 proteins bound to laminin (Lm) and fibronectin (Fn) but not to plasminogen. Moreover, higher levels of adherence to Lm and Fn were detected in parasites grown under HG conditions than in those grown under GR conditions. Furthermore, pretreatment of trichomonads with an anti-*Tv*TIMr polyclonal antibody or pretreatment of Lm- or Fn-coated wells with both recombinant proteins (*Tv*TIM1r and *Tv*TIM2r) specifically reduced the binding of live parasites to Lm and Fn in a concentration-dependent manner. Moreover, *T. vaginalis* was exposed to different glucose concentrations during vaginal infection of women with trichomoniasis. Our data indicate that *Tv*TIM is a surface-associated protein under HG conditions that mediates specific binding to Lm and Fn as a novel virulence factor of *T. vaginalis*.

Trichomonas vaginalis is a protozoan parasite responsible for human trichomoniasis, the most common nonviral sexually transmitted infection, which affects over 276 million people annually worldwide (1). Infection with this organism is associated with severe health complications, such as vaginitis, preterm delivery, urethritis, prostatitis, infertility, and increases in the risks of prostate and cervical cancer. It has also been implicated in facilitating the infection and transmission of human immunodeficiency virus (HIV) (2–4).

To establish an infection in the vagina, *T. vaginalis* must cross the vaginal mucus, adhere to the vaginal and cervical epithelia, and multiply in and colonize the urogenital tract (2, 5). The vagina is one of the most complex mucosal microenvironments and is constantly changing during the menstrual cycle. However, *in vitro* studies have shown that *T. vaginalis* adapts and responds to these changes, modulating the expression of multiple genes, including those encoding virulence factors, to maintain a chronic infection (6).

Energy generation is vital to the maintenance of chronic infection and depends on the availability of nutrients, such as iron and a carbon source. For *T. vaginalis*, glucose is the major energy source under both anaerobic and aerobic conditions. Within the cytoplasm, glycolysis is the initial step of the breakdown of glucose to pyruvate. Pyruvate is metabolized by fermentative oxidation in the hydrogenosome, which generates ATP through substrate-level phosphorylation (7).

These energetic pathways are regulated by the activity of multiple enzymes, some of which are classified as "moonlight-ing" proteins that have alternative functions in the host-parasite relationship of *T. vaginalis*. For example, several hydrogenosomal enzymes (pyruvate:ferredoxin oxidoreductase [PFO]/AP120, malic enzyme/AP65, and α- and β-succinyl-coenzyme A [CoA] synthetase subunits/AP33 and AP51, respectively) can switch functions, depending on their cellular localizations, acting as metabolic enzymes in the hydrogenosome and cytoplasm or as adhesins on the parasite surface (8–10). Importantly, iron and cellular contact positively regulate the level of adherence by directly increasing adhesin synthesis (10).

Other cytoplasmic glycolytic enzymes of *T. vaginalis*, such as glyceraldehyde-3-phosphate dehydrogenase (*Tv*GAPDH) and α-enolase (*Tv*ENO-1), are also moonlighting proteins with dual functions depending on their cellular localization. On the surface of *T. vaginalis*, *Tv*GAPDH functions as a fibronectin (Fn)-binding protein under iron-rich conditions (11), whereas TvENO-1 func-

tions as a plasminogen (Plg)-binding protein during cellular contact (12). Both *Tv*GAPDH and *Tv*ENO-1 play important roles in supporting colonization and persistence in the urogenital tract in different host environments. In spite of multiple reports in which dual localization and novel functions were demonstrated for metabolic enzymes such as those also described for *T. vaginalis*, these trichomonad proteins are considered controversial surface-associated proteins due to the lack of transmembrane domains (TMDs) and/or signal peptides (SPs), the typical characteristics of the integral membrane proteins (13). In addition, a list of moonlighting proteins was recently updated by Amblee and Jeffery (14) and included the GAPDH and the AP120/PFO adhesin. With regard to the majority of the identified moonlighting proteins of other organisms, one of the open avenues of investigation is to identify the pathway that these molecules, including the proteins described for *T. vaginalis*, follow to relocalize to the cell surface to perform a new function.

Triosephosphate isomerase (TIM) is a cytoplasmic glycolytic enzyme involved in the reversible interconversion of dihydroxyacetone phosphate (DHAP) and glyceraldehyde-3-phosphate (G3P), and it plays essential roles in glycolysis (Embden-Meyerhof-Parnas pathway), gluconeogenesis, and the pentose phosphate pathways (15). TIM is an important virulence factor when localized to the cellular surfaces of pathogenic organisms. For example, it is an adhesin for epithelial cells and a laminin (Lm)- and Fn-binding protein during the parasitic phase of *Paracoccidioides brasiliensis* (16). Similarly, TIM is a Plg-binding protein in *Staphylococcus aureus* (17). Moreover, TIM has extracellular functions in parasitic helminths; i.e., it is secreted during infection by *Brugia malayi* and *Schistosoma mansoni* and acts as an antibody target during infection, and it has been considered a potential target for drug and/or vaccine development (18–20). TIM can also acquire functional diversity as a result of gene duplication. In the majority of organisms, it is encoded by a single gene; however, in plants, it is encoded by two *tim* genes that are differentially expressed in the cytosol and the chloroplasts (21). Similarly, in the bacterium *Sinorhizobium meliloti*, TIM is also encoded by two *tim* genes, one involved in erythritol catabolism and the other functioning in gluconeogenesis (22).

In *T. vaginalis*, TIM is encoded by two functional *tvtim* genes (*tvtim1* and *tvtim2*) that are translated into two 27-kDa proteins (*Tv*TIM1 and *Tv*TIM2). The two proteins were recently identified and characterized as recombinant proteins, and their crystal structure and stability were determined (23, 24). *Tv*TIM1 and *Tv*TIM2 are dimeric proteins of 254 amino acids in length. Despite a difference of only four amino acids between these two proteins, the difference significantly affects their structural stability. The *Tv*TIM1r dimer is more stable and less dissociable than the *Tv*TIM2r dimer, which is easily dissociable, suggesting that these changes could directly affect protein function (23, 24). *Tv*TIMs exhibit dual cellular localizations (in the cytoplasm and on the surface of *T. vaginalis*) under regular growth conditions, suggesting that these proteins could have alternative novel functions when they are localized to the parasite surface (24). Evidence suggests that in addition to their enzymatic activities, these two proteins could also have alternative functions in the parasite. For example, recent transcriptomic analyses have reported that *tvtim2* is highly expressed in amoeboid parasites upon binding to Fn (25) as well as in parasites grown under glucose-rich, i.e., high-glucose (HG), conditions compared with *tvtim1* (26). Taken together,

these data suggest that *Tv*TIM could be an additional moonlighting metabolic enzyme in *T. vaginalis*. Thus, the main goal of this study was to identify the novel functions of *Tv*TIM localized to the *T. vaginalis* surface and the effect of glucose on its expression and surface localization. Our results showed that *Tv*TIM is a glycolytic enzyme that is positively regulated by glucose and is localized to the cytoplasm and on the surface of *T. vaginalis*, where it functions as an Lm- and Fn-binding protein under HG conditions.

MATERIALS AND METHODS

***T. vaginalis* culture.** *T. vaginalis* parasites from the fresh clinical isolate CNCD188 (9) were maintained for 3 days by daily passaging in Trypticase-yeast extract-glucose (TYG) medium (modified TYM medium) supplemented with 10% heat-inactivated bovine serum (HIBS) and 25 mM glucose (normal glucose [NG]) at 37°C. For growing the parasites in different glucose concentrations, TYG-HIBS medium was either supplemented with 50 mM glucose (glucose rich [HG]) or not supplemented with glucose, so that only ≤1 mM glucose was present, which was derived from medium components (glucose restricted [GR]). Glucose measurements were verified by the automated glucose-hexokinase method (26) (clinical diagnostic laboratory, MICRO-TEC, Mexico City, Mexico).

Growth kinetics. To assess growth kinetics, 1×10^6 parasites were grown in 5 ml of HG, NG, or GR TYG-HIBS medium. The cultures were incubated at 37°C, and the cell density was determined at 6-h intervals during 24 h of growth using a hemocytometer counting method. Regular TYM (13 mM maltose) was used as a normal growth control (27). Cell viability was monitored by the trypan blue exclusion method.

RNA isolation and reverse transcription (RT)-PCR analysis. Total RNA was isolated from parasites (2×10^7) grown under GR, NG, or HG conditions using TRIzol reagent (Invitrogen, Carlsbad, CA). To obtain cDNA, 5 µg of total RNA was treated with DNase I (3 U) and reverse transcribed using a RevertAid first-strand cDNA synthesis kit (Thermo Scientific-Pierce, Rockford, IL) and oligo(dT) primers, as recommended by the manufacturer. For PCR amplification, 500 ng of cDNA, *Taq* DNA polymerase (Invitrogen), and primers specific for the reported sequences in TRICHDB for the *tvtim1* (TVAG_497370) and *tvtim2* (TVAG_096350) genes were used, as previously described (23). The *tvtim1* primers were 5′-ACATTCTTTGTCGGAGGC-3′ (sense) and 5′-AATGTTGATGAAACCTGG-3′ (antisense), and the *tvtim2* primers were 5′-ACATTCTTCGTCGGTGGT-3′ (sense) and 5′-AATGTTGATGAAGCCTGG-3′ (antisense). A 726-bp fragment was amplified for both the *tvtim1* and *tvtim2* genes. The amplification program consisted of 25 cycles of denaturation at 94°C for 1 min, annealing at 55°C for 1 min, and extension at 72°C for 1 min. The 112-bp amplicon of the β-tubulin gene of *T. vaginalis* (28) was used as an internal control. These experiments were performed at least three independent times, with similar results.

WB analysis. Total protein extracts from *T. vaginalis* (2×10^7) grown under GR, NG, or HG conditions were obtained using a previously described method (8, 9). Briefly, the parasites were resuspended in 500 µl of NET (50 mM Tris-HCl, 150 mM NaCl and 5 mM EDTA) buffer (pH 7.4) in the presence of proteinase inhibitors (1 mM Nα-*p*-tosyl-L-lysine chloromethyl ketone [TLCK] and 0.2 mM leupeptin), lysed with 0.5% deoxycholic acid (DOC) for 20 min at 4°C, and then brought up to a final volume of 1 ml with TDSET (10 mM Tris-Cl [pH 7.8], 0.2% DOC, 0.1% SDS, 10 mM EDTA, and 1% Triton X-100) buffer. The lysate was layered on a sucrose cushion and centrifuged at $16,000 \times g$ for 30 min at 4°C. Protein extracts (supernatants) were analyzed by SDS-PAGE, blotted onto a nitrocellulose (NC) membrane (0.2 µm pore size; Bio-Rad Laboratories, Hercules, CA), blocked with 10% nonfat dried milk in phosphate-buffered saline (PBS)–0.1% Tween 20 (PBS-T) overnight at 4°C, washed with PBS-T, and incubated with different primary antibodies for 18 h at 4°C. After incubation for 2 h at room temperature with a peroxidase-conjugated goat anti-rabbit secondary antibody (1:3,000 dilution; Bio-Rad), reactive bands were developed using a chemiluminescence system (SuperSignal West Pico chemiluminescent substrate; Thermo Scien-

tific-Pierce). Images were captured with a ChemiDoc XRS system (Bio-Rad) and analyzed using Quantity One software (Bio-Rad). Preimmune (PI) serum was used as a negative control, and other primary antibodies were used to detect *Tv*TIM and the control proteins in Western blotting (WB), including the following: anti-*Tv*TIMr, an antibody previously generated against the recombinant *Tv*TIM2 protein that recognizes both recombinant *Tv*TIM proteins (23); anti-AP65, an antibody generated against the native AP65 trichomonad adhesin; anti-EhHKr, an antibody generated against the *Entamoeba histolytica* recombinant hexokinase that cross-reacts with *T. vaginalis* hexokinase (*Tv*HK); and anti-*Tv*ENOr, an antibody generated against the recombinant *T. vaginalis* alpha-enolase (*Tv*ENO; TVAG_329460). The control proteins included the loading control; the adhesin AP65; TvHK, which is upregulated by glucose; and *Tv*ENO, which is not affected by glucose (12, 29, 30). These experiments were performed at least three independent times, with similar results.

Immunolocalization of *Tv*TIM. To determine the localization of *Tv*TIM in *T. vaginalis* grown under different glucose conditions (GR and HG), indirect immunofluorescence assays and confocal microscopy analysis were performed. Parasites were cultured on coverslips for 20 h at 37°C and fixed with 2% paraformaldehyde in PBS for 30 min at room temperature. We used a type of fixation that produces a partial permeabilization of cells, which allowed us to identify both intracellular and surface-associated localization in the same parasite, as previously reported (31). The parasites were washed with 1% bovine serum albumin (BSA) in PBS and blocked with 0.5 M glycine for 1 h and 1% fetal bovine serum for 15 min at room temperature. The parasites were incubated with an anti-*Tv*TIMr antibody or PI serum (both at a 1:50 dilution) for 16 h at 4°C, washed five times with PBS, and incubated with a fluorescein isothiocyanate (FITC)-conjugated anti-rabbit secondary antibody (1:100 dilution) (Thermo Scientific-Pierce) for 2 h at room temperature. The parasite surface phospholipids were stained with DIL (DIL-CM-38 at a 1:2,000 dilution; Molecular Probes-Invitrogen) for 30 min at room temperature. To label the nuclei, the coverslips were mounted with Vectashield–4′,6-diamidino-2-phenylindole (DAPI) mounting solution (Vector Laboratories, Burlingame, CA), and the parasites were analyzed by confocal microscopy using a Zeiss microscope and ZEN 2012 software (Carl Zeiss, Germany). These experiments were performed at least three independent times, with similar results.

To confirm the glucose effect on the localization of *Tv*TIM to the surface of *T. vaginalis*, parasites were maintained for 3 days by daily passaging under GR conditions before supplementation with different glucose concentrations (≤1, 2.5, 5, 10, 25, and 50 mM) on coverslips for 1 h at 37°C. After that, the same protocols as described above for indirect immunofluorescence assays and confocal microscopy analyses were performed.

Immunogold labeling and transmission electron microscopy. For immunogold labeling assays, parasites grown in HG medium for 20 h at 37°C were fixed with 4% paraformaldehyde–0.2% glutaraldehyde in serum-free Dulbecco modified Eagle medium (DMEM). Afterward, the parasites were dehydrated in ethanol and embedded in LR white resin (London Resin Co. Ltd., United Kingdom), and then the parasite samples were polymerized under UV light at 4°C overnight. Ultrathin sections were mounted on mesh nickel grids and incubated with the anti-*Tv*TIMr antibody (1:30 dilution) overnight. After several washes in 1% PBS–BSA, the sections were incubated with secondary 10- or 20-nm gold-conjugated goat anti-rabbit IgG (Ted Pella, Inc., USA) for 1 h at room temperature. Parasites incubated only with secondary antibody conjugated to gold particles were used as a negative control. Ultrathin sections were analyzed by transmission electron microscopy (TEM) using a JEOL JEM-1011 transmission electron microscope (JEOL Ltd., Tokyo, Japan).

Affinity ligand assays. To determine the binding of the recombinant *Tv*TIM proteins (*Tv*TIM1r and *Tv*TIM2r) to Lm, Fn, and Plg, far-Western blotting (FWB) assays were performed as previously described (16), with minor modifications. *Tv*TIM1r and *Tv*TIM2r (1 μg) were subjected to SDS-PAGE, blotted onto NC membranes (0.2-μm pore size; Bio-Rad),

and blocked with 10% nonfat dried milk in PBS-T overnight at 4°C. The blots were washed with PBS-T and incubated with Lm from Engelbreth-Holm-Swarm murine sarcoma basement membrane (L2020; Sigma Co., St. Louis, MO), Fn from human plasma (F2006; Sigma), human Plg (STA-239; Cell Bio-Labs, San Diego, CA), or pp*Tv*CP4r (32) (an unrelated protein used as a negative control) (30 μg ml⁻¹ each) in PBS-T–1% BSA (PBS-T–BSA) overnight at 4°C. The blots were then washed extensively with PBS-T and incubated overnight at 4°C with the corresponding anti-Lm (L9393; Sigma), anti-Fn (F3348; Sigma), anti-Plg (STA-139; Cell Bio-Labs), or anti-pp*Tv*CP4r (32) primary antibody in PBS-T–BSA (all at 1:1,000 dilutions). The blots were washed extensively with PBS-T and incubated for 2 h at room temperature with a peroxidase-conjugated goat anti-rabbit or donkey anti-goat secondary antibody (1:3,000 or 1:2,000 dilution, respectively; Bio-Rad or Jackson ImmunoResearch, West Grove, PA). Reactive bands were developed using a chemiluminescence system (Thermo Scientific-Pierce). Images were captured with a ChemiDoc XRS system (Bio-Rad) and analyzed with Quantity One software (Bio-Rad). A recombinant alpha-enolase protein (*Tv*ENOr) previously shown to interact with Plg (12) was obtained by cloning the TVAG_329460 gene into the pET19b plasmid, expressed in the *E. coli* BL21(DE3) Star Rosetta II strain, affinity purified by immobilized-metal affinity chromatography (IMAC) and used as an FWB positive control (23). The unrelated recombinant protein pp*Tv*CP4r was used as an FWB negative control (32). A WB assay of the Lm, Fn, and Plg proteins directly incubated with a secondary antibody conjugated to peroxidase was used as an additional negative control to evaluate the presence of nonspecific binding of the secondary antibody to the Lm, Fn, and Plg proteins. *Tv*TIM1r and *Tv*TIM2r were directly incubated with an anti-Lm, anti-Fn, anti-Plg, or anti-pp*Tv*CP4r antibody as other negative controls for specificity. As positive controls, *Tv*TIM1r, *Tv*TIM2r, *Tv*ENOr, or pp*Tv*CP4r was directly incubated with the corresponding anti-*Tv*TIMr (1:1,500 dilution), anti-*Tv*ENOr (1:2,000 dilution), or anti-pp*Tv*CP4r (1:2,000 dilution) antibodies. These experiments were performed at least three independent times, with similar results.

Dot blot binding assays. Dot blot binding assays were performed to confirm the abilities of the recombinant *Tv*TIM proteins to bind to Lm and Fn but not to Plg. Different amounts (0, 0.1, 0.3, 0.5, 1.0, 2.0, and 4.0 μg) of *Tv*TIM1r and *Tv*TIM2r were transferred onto NC membranes (0.2-μm pore size; Bio-Rad) using a Bio-Dot microfiltration blotting device (Bio-Rad). The membranes were blocked with 5% skim milk in Tris-buffered saline–Tween 20 (0.1%) (TBS-T) overnight at 4°C, washed with TBS-T, and incubated with Lm, Fn (30 μg ml⁻¹ [*Tv*TIM1r, *Tv*TIM2r, and *Tv*CP4r]), or Plg (30 μg ml⁻¹ [*Tv*TIM1r, *Tv*TIM2r, *Tv*ENO, and *Tv*CP4r] and 60 μg ml⁻¹ [*Tv*TIM1r and *Tv*TIM2r]) in TBS-T-BSA with gentle shaking overnight at 4°C. After extensive washing with TBS-T, the blots were incubated with the corresponding primary antibody (anti-Lm, anti-Fn, or anti-Plg; 1:1,000 dilution) in TBS-T overnight at 4°C, washed, and incubated for 2 h at room temperature with a peroxidase-conjugated goat anti-rabbit or donkey anti-goat secondary antibody (1:3,000 or 1:2,000 dilution; Bio-Rad or Jackson ImmunoResearch, respectively). Reactive spots were developed using a chemiluminescence system (Thermo Scientific-Pierce). Images were captured with a ChemiDoc XRS system (Bio-Rad) and analyzed using Quantity One software (Bio-Rad). As dot blot positive and negative controls, different amounts of *Tv*TIM1r and *Tv*TIM2r, or *Tv*CP4r (33) as an unrelated protein, were directly incubated with anti-*Tv*TIMr or anti-*Tv*CP4r antibody, respectively. Additional positive (*Tv*ENOr) and negative (*Tv*CP4r) controls were used for the dot blot binding assays. The experiments were performed at least three independent times, with similar results.

Fn and Lm binding assays. For Fn and Lm binding assays, 96-well microtiter plates (Jet Biofilm, USA) were coated with Lm or Fn (2 μg per well) diluted in carbonate buffer (pH 9.6) overnight at 4°C. The wells were washed five times with PBS-T, blocked with 5% skim milk in PBS-T for 2 h at room temperature, and washed five times with PBS-T. To verify that the wells were coated with Fn or Lm, incubation with an anti-Lm or anti-Fn antibody (both at a 1:200 dilution) followed by a FITC-conju-

gated secondary anti-rabbit antibody was performed. The fluorescence emission per well was quantified at 520 nm by using a Gemini EM spectrofluorometer (Molecular Devices SpectraMax) and indicated that wells were completely coated with Lm or Fn (data not shown). BSA (2 μg per well), an unrelated protein, was also used to coat the 96-well microtiter plates as an additional control for parasite binding specificity.

To determine the effects of glucose on the binding of *T. vaginalis* to Lm and Fn, adherence assays using live parasites grown under GR, NG, and HG conditions were performed. The parasites (1×10^6 parasites ml^{-1}) were resuspended in serum-free TYG medium, labeled with 75 μM Cell-Tracker Blue CMAC (CTB; Molecular Probes, OR) for 45 min at 37°C with gentle shaking (100 rpm), and then washed extensively with TYG medium supplemented with 10% HIBS. Labeled parasites (5×10^5 per well) from each glucose condition were added to microtiter wells coated with 2 μg of Lm, Fn, or BSA and incubated for 30 min at 37°C. Unbound parasites were removed, the wells were washed with PBS, and the fluorescence emission from the parasites attached to Lm, Fn, or BSA was quantified at 466 nm with a Gemini EM spectrofluorometer (Molecular Devices SpectraMax) and taken as the value for 100% attached parasites under each glucose condition. For the protein binding inhibition assays, labeled parasites grown under HG conditions were preincubated with anti-*Tv*TIM IgGs (0, 100, 200, 300, and 400 μg ml^{-1}) for 30 min at 4°C. The same concentrations of PI rabbit serum or anti-pp*Tv*CP4r IgGs were used as negative controls. Untreated parasites were taken as 100% attached parasites. The experiment was performed in triplicate at least three independent times, with similar results. Another inhibition experiment was performed using the recombinant *Tv*TIM proteins as competitors. The Lm- or Fn-coated wells were preincubated for 1 h at 4°C with increasing amounts (0 to 1.6 μg) of the *Tv*TIM1r or *Tv*TIM2r protein to compete for the specific binding of trichomonads to these ECM proteins. Then, live parasites grown under HG conditions were added to the wells and incubated for 30 min at 37°C. The same amounts of the unrelated recombinant protein pp*Tv*CP4r were used as negative competitor controls.

Glucose concentration measurement in VSs. To determine the glucose concentrations in vaginal secretions (VSs) from women with trichomoniasis, a total of 85 samples were included in this study. The VSs were obtained from women who were enrolled at the Hospital General de Mexico under an institutional review board (IRB)-approved protocol (DI/14/204/03/010) and who provided written informed consent. The enrolled subjects had received the diagnosis of cervicovaginitis and other gynecological disorders as determined by clinical examination. The VSs were collected from vaginal discharge using sterile cotton swabs, and the samples were diluted in saline solution (at a 1:5 dilution). The presence of cellular components such as vaginal epithelial cells (VECs), white blood cells (WBCs), bacteria, and yeasts was determined by microscopic analysis. The pH was determined using indicator strips with pH ranges of 0 to 14 and 4 to 7 (ColorpHast indicator strips; Merck). The presence of *T. vaginalis* and other pathogens, such as *Gardnerella vaginalis*, *Candida albicans*, or enterobacteria, was determined by microscopic analysis and *in vitro* culture. For *T. vaginalis* culture, the InPouch Tv test (Biomed Diagnostic, White City, OR) was used. To determine the glucose concentration in the VS samples, the samples were clarified by centrifugation at 12,000 × *g* for 5 min at 4°C, the supernatants were transferred to new microtubes, and glucose measurements were performed by the glucose-hexokinase automated method (MICRO-TEC).

Statistical analysis. Statistically significant differences between means were determined by analysis of variance (ANOVA) using GraphPad Prism 5.0. The data were analyzed by one-way ANOVA using the Tukey method comparing all pairs of columns ($P < 0.05$) for Fig. 1 and 5 to 7. The scores showing statistical significance are indicated in the figures with asterisks. The corresponding *P* values are indicated in the figure legends.

RESULTS

Glucose promotes the growth of *T. vaginalis*. To assess the growth of *T. vaginalis* in different glucose concentrations, we per-

formed growth kinetic assays using *T. vaginalis* parasites from the fresh clinical isolate CNCD188 grown under GR, NG, or HG conditions. Parasite numbers were counted at 6-h intervals for 24 h. The parasites grown under HG conditions reached a cellular density at 24 h of $4.78 \times 10^6 \pm 0.16 \times 10^6$ cells ml^{-1}, compared with $3.73 \times 10^6 \pm 0.06 \times 10^6$ cells ml^{-1} and $1.97 \times 10^6 \pm 0.14 \times 10^6$ cells ml^{-1} for those grown under NG and GR conditions, respectively, and $3.78 \times 10^6 \pm 0.12 \times 10^6$ cells ml^{-1} for those grown in regular TYM medium (Fig. 1A1). Cell viability was monitored by the trypan blue exclusion method and showed that the numbers of viable cells did not significantly differ between the parasites grown in the various glucose concentrations and those grown in the control TYM medium (Fig. 1A2). These data also show that the growth of *T. vaginalis* increased significantly with glucose concentration ($P \leq 0.05$) compared with the parasite growth under GR conditions.

Glucose induces differential expression of the *tvtim* genes. To evaluate the effects of glucose on the expression of the *Tv*TIM-encoding genes (*tvtim1* and *tvtim2*), we performed semiquantitative RT-PCR assays (Fig. 1B1) using total RNA isolated from parasites grown under GR, NG, or HG conditions. Densitometric analysis was also performed to assess the differences observed in the amplicons. Our results showed that *tvtim1* was the most highly expressed in the parasites grown under GR conditions (Fig. 1B1, lane 1) and *tvtim2* was overexpressed in the parasites grown under HG conditions (Fig. 1B1, lane 3). These differences were corroborated by densitometric analysis of the amplicons (Fig. 1B2) normalized against the β-tubulin amplicon for each glucose concentration. The differences were significant ($P < 0.05$ [Fig. 1B2]), demonstrating that the *tvtim* genes were differentially expressed in *T. vaginalis*, depending on the glucose concentration.

Expression of *Tv*TIM is upregulated by glucose. To determine the effects of glucose on the protein expression of *Tv*TIM, total protein extracts from parasites grown under different glucose conditions were analyzed by WB assays using an anti-*Tv*TIMr antibody that recognizes a 27-kDa band corresponding to both *Tv*TIM proteins of *T. vaginalis*. Our results showed an increase in the amount of the *Tv*TIM band in the parasites grown under NG and HG conditions (Fig. 1C1, lanes 2 and 3, respectively) compared with those grown under GR conditions (Fig. 1C1, lane 1). These differences were corroborated by densitometric analysis of the bands detected by WB normalized against the AP65 band (Fig. 1C1) and were found to be significant ($P < 0.05$) (Fig. 1C2). To confirm that glucose affected the expression of other trichomonad glycolytic enzymes, such as hexokinase (*Tv*HK) and enolase (*Tv*ENO), which participate in the first and ninth reactions of the glycolytic pathway, respectively, WB assays were also performed using the same protein extracts from the parasites grown under different glucose conditions. The expression of *Tv*ENO did not change (Fig. 1C1), whereas similar to *Tv*TIM expression, the expression of *Tv*HK exhibited a marked increase in the parasites grown under HG conditions (Fig. 1C1, lane 3) compared with those grown under GR conditions (Fig. 1C1, lane 1). These differences were corroborated by densitometric analysis of the bands detected by WB normalized against the AP65 band (Fig. 1C2) and were found to be significant ($P < 0.05$) for *Tv*HK but not for *Tv*ENO. These data showed that *Tv*TIM and *Tv*HK, two glycolytic enzymes of *T. vaginalis*, are modulated by the glucose concentrations, whereas *Tv*ENO and AP65 are not affected by glucose levels.

_Tv_TIM surface localization is affected by glucose. To assess
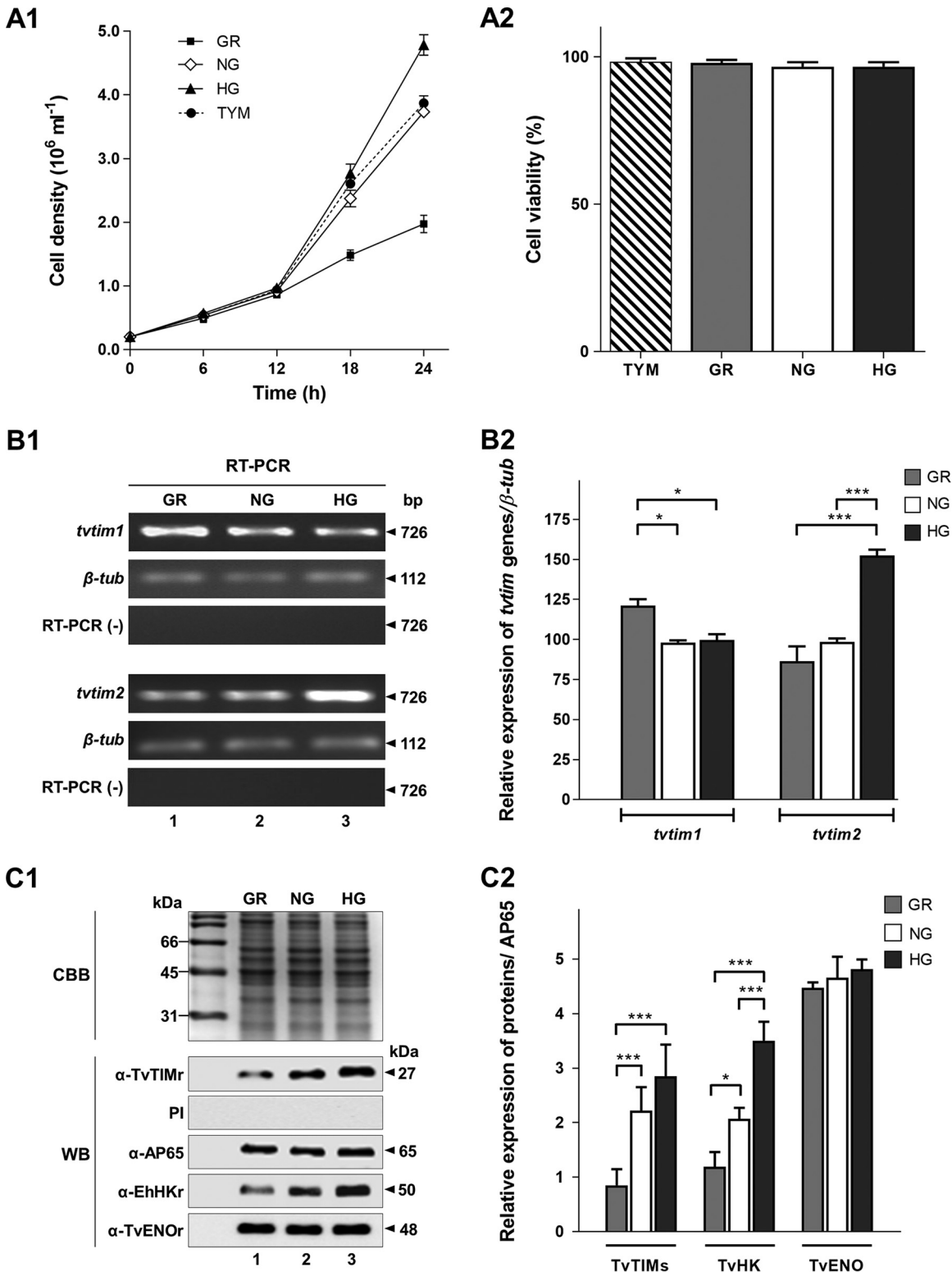
FIG 1 Glucose promotes the growth of *Trichomonas vaginalis* and differentially modulates *tvtim1* and *tvtim2* gene expression and amount of *Tv*TIM. (A1) Effects of GR (≤1 mM), NG (25 mM) and HG (50 mM) conditions on *T. vaginalis* growth. The initial number of parasites cultivated under the different glucose conditions was 2×10^5 cells ml^{-1}. TYM (13 mM maltose) regular medium was used as a normal growth control. Cell density was determined at 6-h intervals during 24 h of growth at 37°C. (A2) Cell viability was monitored by trypan blue exclusion via hemocytometer counts after 24 h of incubation. All data (A1 and A2) are the means ± SDs of three independent experiments in duplicates. (B1) Semiquantitative RT-PCR using primers specific for the *tvtim1* and *tvtim2* genes (726 bp) and cDNA from parasites grown under GR (lane 1), NG (lane 2), and HG (lane 3) conditions. The β-tubulin gene (β-*tub*; 112 bp) was amplified as an internal control, using the cDNA from the parasites grown under different glucose conditions. RT-PCR was the negative (−) control, for which DNase-treated RNA without reverse transcriptase was used as a template. The sizes of the amplicons are given in base pairs. (B2) Densitometric analysis of the RT-PCR

the cellular localization of *Tv*TIM in trichomonads grown under different glucose conditions, we performed indirect immunofluorescence assays on paraformaldehyde-fixed parasites, using an anti-*Tv*TIMr antibody. The images were analyzed by confocal microscopy. Consistent with the WB data, Fig. 2A shows the increased fluorescence intensity of cytoplasmic and surface-associated *Tv*TIM (in green; panels d and i), which colocalized with the membrane marker (Dil, in red; panels c and h) as yellow label (merge; panels e and j) of parasites grown under HG conditions (Fig. 2A, panels a to e) compared with those grown under GR conditions (Fig. 2A, panels f to j), which showed a reduced green fluorescent signal in the cytoplasm and parasite surface (Fig. 2A, panels i and j). In those grown under HG conditions but treated with PI serum, used as a negative control (Fig. 2A, panels k to o), no green fluorescent signal was observed, as expected. Thus, *Tv*TIM showed a patchy distribution and colocalization (in yellow) on the surface of parasites grown under HG conditions (Fig. 2A, panels a to e), while those grown under GR conditions showed less *Tv*TIM on the cell surface (Fig. 2A, panels f to j). These data suggest that in *T. vaginalis*, the amount and surface localization of *Tv*TIM are positively regulated by glucose.

Our next goal was to confirm the glucose effect on the localization of *Tv*TIM to the surface of *T. vaginalis*. Thus, we performed indirect immunofluorescence assays on paraformaldehyde-fixed parasites grown in different glucose concentrations ($\leq$1, 2.5, 5, 10, 25, and 50 mM) for 1 h, supplemented after glucose starvation. Figure 2B shows that *Tv*TIM localized on the surface of *T. vaginalis* after 1 h of glucose supplementation; this is better visualized at 25 and 50 mM glucose (Fig. 2B, panels q to t and u to x, respectively), with colocalization points in yellow that increased proportionally to the glucose concentration up to ~3-fold. The coefficient of colocalization varied from 6.5% at $\leq$1 mM glucose (10.2% and 10.8% at 2.5 and 5.0 mM glucose and 14.9% and 15.8% at 10 and 25 mM glucose, respectively) to 16.8% at 50 mM glucose (Fig. 2B, panels h, l, p, t, and x). These data suggest that in *T. vaginalis*, the amount and surface localization of *Tv*TIM are positively regulated by glucose. Thus, our next aim was to identify the possible pathway followed by *Tv*TIM to the parasite surface under HG conditions.

_Tv_TIM follows an unconventional pathway to the surface of _T. vaginalis_ under HG conditions. To explore the possible cellular trafficking pathway of *Tv*TIM to the plasma membrane of *T. vaginalis* despite of the lack of transmembrane domains and signal peptides in the protein, we performed immunogold localization assays on fixed parasites grown under HG conditions using the anti-*Tv*TIMr antibody and transmission electron microscopy
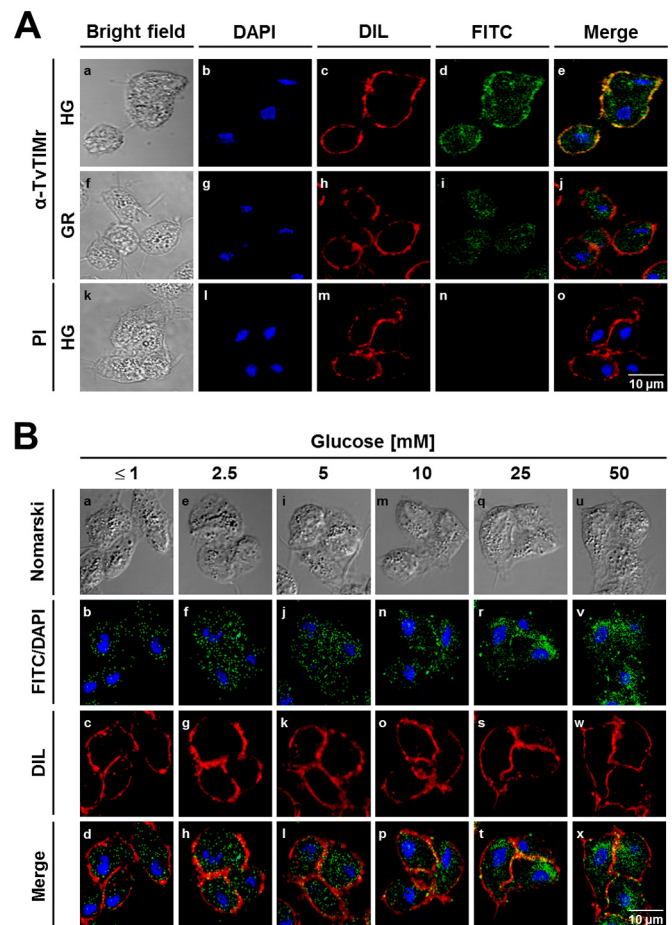
FIG 2 Glucose promotes the localization of *Tv*TIM to the surface of *T. vaginalis*. (A) Indirect immunofluorescence and bright-field microscopy showed the cytoplasmic and surface localization and expression of *Tv*TIM in parasites grown under HG (a to e) and GR (f to j) conditions for 24 h at 37°C. Paraformaldehyde-fixed parasites were incubated with a primary anti-*Tv*TIMr antibody (1:50 dilution) followed by a FITC-conjugated secondary antibody (1:100 dilution). Parasites grown in HG were incubated with preimmune (PI) rabbit serum (1:50 dilution) followed by a FITC-conjugated secondary antibody as a negative control (k to o). (B) Cytoplasmic and surface localization of *Tv*TIM in parasites grown in increasing glucose concentrations ($\leq$1, 2.5, 5, 10, 25, and 50 mM) for 1 h at 37°C. Paraformaldehyde-fixed parasites were incubated with a primary anti-*Tv*TIMr antibody (1:50 dilution) followed by a FITC-conjugated secondary antibody (1:100 dilution). In both panels A and B, the confocal microscopy (Zeiss) images show *Tv*TIM labeled with FITC (in green), nuclei labeled with DAPI (in blue), and the parasite membrane labeled with DIL (1:2,000 dilution, in red). The merged images show colocalization between the *Tv*TIM protein and the parasite surface in yellow. Bar size: 10 μm. These experiments were performed three independent times, with similar results.

amplicons, as detected by ethidium bromide staining after electrophoresis in 1% agarose gels in panel B1 performed using Quantity One software (Bio-Rad). The bar graphs show the relative amounts of *tvtim1* and *tvtim2* transcripts normalized to the β-tubulin gene transcript level. The error bars indicate SDs, determined from three independent experiments. The asterisks (* and ***) show the significant differences ($P < 0.05$) of the amplicons obtained under the three glucose conditions for each *tvtim* gene as determined by ANOVA. (C1) SDS-PAGE and Coomassie brilliant blue (CBB) staining of 12% polyacrylamide gels were performed to assess the total protein extracts from parasites grown under GR (lane 1), NG (lane 2), and HG (lane 3) conditions. For WB assays, duplicated gels from panel C1 transferred onto NC membranes were incubated with different antibodies, including an anti-*Tv*TIMr antibody (1:1,000 dilution) that recognized a 27-kDa band corresponding to the native *Tv*TIM proteins. An anti-AP65 adhesin (anti-AP65) antibody (1:1,500 dilution) that recognized a 65-kDa band was used as a loading control, and preimmune rabbit serum (PI) (1:1,500 dilution) was used as a negative control. An anti-*Entamoeba histolytica* hexokinase (α-EhHKr) antibody (1:1,000 dilution) that recognized a 50-kDa band in *T. vaginalis* that corresponds to the *T. vaginalis* hexokinase (*Tv*HK) was used as a control for glucose-induced modulation. An anti-enolase (α-*Tv*ENOr) antibody (1:1,500 dilution) that recognized a 48-kDa band was used as a control for the absence of glucose-induced effects. (C2) Densitometric analysis of the bands detected by WB (C1) performed with Quantity One software (Bio-Rad). The bar graphs show the relative amounts of *Tv*TIM, *Tv*HK, and *Tv*ENO proteins normalized to the level of the AP65 protein, which was used as a loading control. The error bars indicate the SDs of three independent experiments. The asterisks (* and ***) show significant differences ($P < 0.05$) among the protein bands detected by the antibodies under HG and NG conditions compared with GR conditions, as determined by ANOVA.

A

B
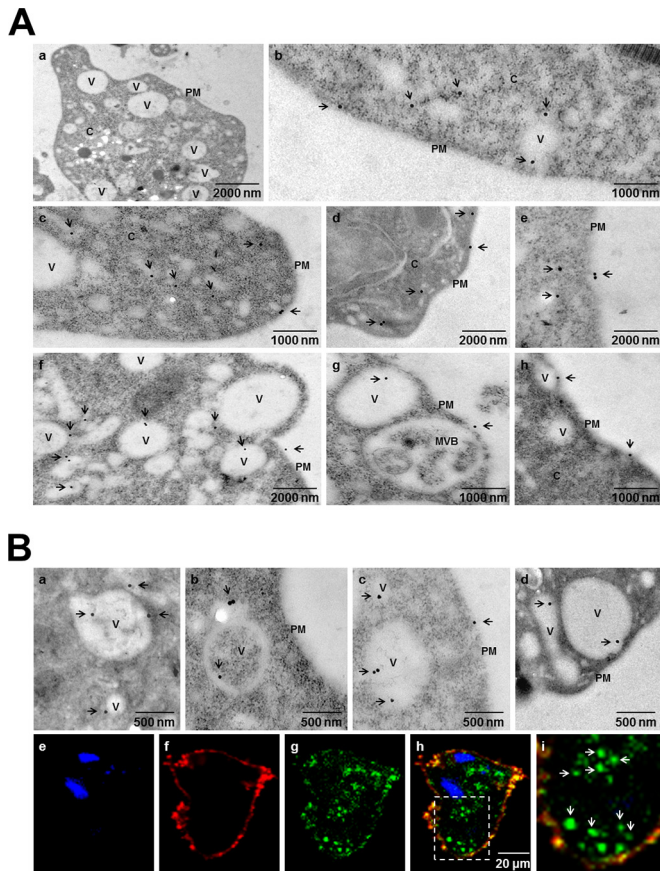
FIG 3 *Tv*TIM shows two possible unconventional trafficking routes to the plasma membrane under HG conditions. (A) Immunogold labeling of parasites grown under HG conditions using a primary anti-*Tv*TIMr antibody at a 1:30 dilution and a secondary antibody conjugated to 10- or 20-nm gold particles. The samples were analyzed by TEM. The TEM images show parasites directly incubated with a secondary antibody conjugated to gold particles as a negative control (a). In general, the *Tv*TIM gold labeling shows localization free in the cytoplasm (C), in vacuoles (V), and on the parasite surface, associated with the plasma membrane (PM). Additionally, TEM images show two possible unconventional trafficking routes of *Tv*TIM from the cytoplasm to the plasma membrane (b). Panels c to e show the trafficking of *Tv*TIM to the plasma membrane through an unconventional pathway independent of vesicles. Panels f to h show the trafficking of *Tv*TIM to the plasma membrane through an unconventional pathway dependent on vesicles or multivesicular body (MVB)-like structures. The arrows point to the gold particles. (B) The TEM images show *Tv*TIM labeling localized on the inner or outer face of the vesicle membranes (a). *Tv*TIM labeling also localized in vesicles with or without cytoplasmic content and near the plasma membrane (b and c). *Tv*TIM labeling also localized in vesicles that were in the process of fusing with the plasma membrane (d). Bar size: 500 nm. The confocal microscopy images show the green *Tv*TIM label in compartments similar to cytoplasmic vesicles, vesicles near the plasma membrane, and vesicles in the process of fusion with the plasma membrane (g to i). The images show *Tv*TIM labeled with FITC (g; in green), nuclei labeled with DAPI (e; in blue), and the parasite membrane labeled with DIL (f; in red). The merged images show colocalization of the *Tv*TIM protein with the parasite surface in yellow (h and i). The arrows point to vesicular structures. The framed region in panel h is magnified in panel i. Bar size: 20 μm.

(TEM). Figure 3 shows the immunogold particles of *Tv*TIM in the cytoplasm, free or inside vacuoles, and on the parasite membrane (Fig. 3A, panel b, arrows). Additionally, we identified two possible unconventional trafficking pathways of *Tv*TIM that could explain its relocalization from the cytoplasm to the parasite membrane,

through a dependent or an independent vesicular unconventional pathway (Fig. 3A, panel b, arrows). *Tv*TIM was detected in a possible trafficking route to the plasma membrane free of cytoplasmic vesicles (Fig. 3A, panel c, arrows); *Tv*TIM signal was also detected close to or exposed on the outer face of the plasma membrane (Fig. 3A, panels d and e, arrows). Moreover, we detected *Tv*TIM signal in different-sized vesicles (Fig. 3A, panel f, arrows), and *Tv*TIM was present in putative secretory vesicles or multivesicular body (MVB)-like structures in the process of being fused with the plasma membrane (Fig. 3B, panels g and h, arrows), in contrast with the negative control, where no gold particles were observed (Fig. 3A, panel a). Figure 3B shows that *Tv*TIM associates with the membranes of vesicles (panel a), in vesicles with or without cytoplasmic content close to the plasma membrane (panels b and c), or in vesicles fused with the plasma membrane (panel d). The localization of *Tv*TIM in vesicles was corroborated by indirect immunofluorescence assays (Fig. 3B, panels e to i). The images show *Tv*TIM (in green) in cytoplasmic vesicles, in vesicles close to the plasma membrane (Fig. 3B, panels g to i), and in merge with DIL (red), a surface marker, in yellow (Fig. 3B, panels h and i). These data suggest the possible unconventional trafficking and secretory pathways followed by *Tv*TIM to relocalize to the plasma membrane under HG conditions. They also suggest that *Tv*TIM could be a multifunctional protein with dual localization modulated by glucose concentration. Thus, our next goal was to determine whether the surface-associated *Tv*TIM is able to bind to extracellular matrix (ECM) proteins such as Lm and Fn or to Plg under HG conditions and play a key role in the host-parasite interaction.

Recombinant *Tv*TIMs bind to ECM proteins. To assess the abilities of recombinant *Tv*TIM proteins (*Tv*TIMr) to bind to Lm, Fn, and Plg (Fig. 4A), we performed FWB assays (Fig. 4C to F). *Tv*TIM1r and *Tv*TIM2r were subjected to SDS-PAGE, electroblotted onto NC membranes, and incubated with Lm, Fn, Plg, or pp*Tv*CP4r (an unrelated protein used as a negative control). Specific protein-protein interactions were detected by WB using an anti-Lm, anti-Fn, anti-Plg, or anti-pp*Tv*CP4r antibody. Figure 4 shows that *Tv*TIM1r and *Tv*TIM2r bound to Lm (Fig. 4C and D, lane 7) and Fn (Fig. 4C and D, lane 8) but not to Plg (Fig. 4C and D, lane 9) or pp*Tv*CP4r (Fig. 4C and D, lane 10). The positive control, *Tv*ENOr, had a positive reaction to Plg (Fig. 4E, lane 8), and the negative control, pp*Tv*CP4r, had no reaction when incubated with the different proteins tested (Fig. 4F, lanes 6 to 8). The WB positive controls were directly incubated with anti-*Tv*TIMr, anti-*Tv*ENOr, or anti-pp*Tv*CP4r antibodies (Fig. 4C to F, lanes 2). An additional negative control (Fig. 4C and D, lanes 3 to 6, and Fig. 4E and F, lanes 3 to 5, respectively) demonstrated that the primary antibodies used that recognized the corresponding proteins by WB (Fig. 4B, lanes 4 to 6) did not cross-react with the recombinant proteins tested (*Tv*TIM1r, *Tv*TIM2r, *Tv*ENOr, and pp*Tv*CP4r), nor did the secondary antibodies conjugated to horseradish peroxidase (HRPO) react with the proteins tested (Lm, Fn, and Plg), as shown in Fig. 4B, lanes 7 to 9.

To confirm the specific binding of recombinant *Tv*TIMs to Lm and Fn and the lack of binding to Plg, dot blot binding assays were performed (Fig. 5). Increasing amounts (0 to 4 μg) of *Tv*TIM1r (Fig. 5A) and *Tv*TIM2r (Fig. 5B) were immobilized onto NC membranes and incubated with (30 μg ml^{-1}) Lm, Fn, or Plg. As positive controls, *Tv*TIM1r and *Tv*TIM2r were directly incubated with anti-*Tv*TIMr antibody. Similarly, protein-protein interactions were detected by WB using anti-Lm, anti-Fn, or anti-Plg
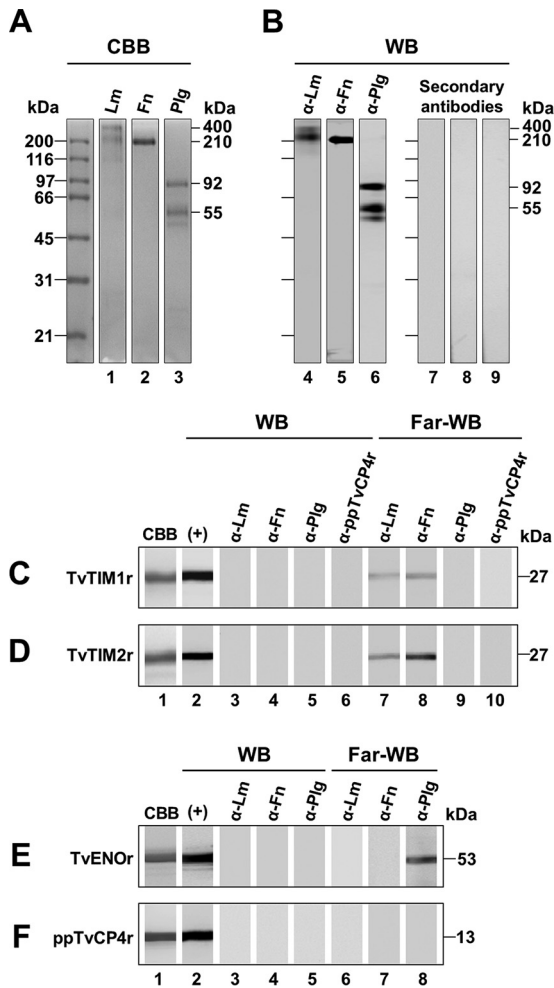
FIG 4 Binding of recombinant *Tv*TIM proteins to ECM components. (A) Electrophoretic analysis of laminin (Lm), fibronectin (Fn), and plasminogen (Plg) proteins. SDS-PAGE and Coomassie brilliant blue (CBB) staining of 10% polyacrylamide gels show the pattern of each protein (lanes 1 to 3). (B) For WB assays, duplicated gels from panel A transferred onto NC membranes were incubated with the specific primary antibodies anti-Lm (lane 4), anti-Fn (lane 5), and anti-Plg (lane 6), followed by incubation with the HRPO-conjugated secondary antibody. Duplicated NC membranes were directly incubated with secondary antibodies conjugated to HRPO, as a negative control for nonspecific signal (lanes 7 to 9). For far-Western blotting assays, the recombinant proteins (1 μg) *Tv*TIM1r (C), *Tv*TIM2r (D), *Tv*ENOr (E), and pp*Tv*CP4r (F) were subjected to SDS-PAGE, blotted onto NC membranes, and incubated with (30 μg ml^{-1}) Lm (C and D, lane 7; E and F, lane 6), Fn (C and D, lane 8; E and F, lane 7), Plg (C and D, lane 9; E and F, lane 8), or pp*Tv*CP4r (C and D, lane 10). The specific protein-protein interactions were detected by WB using the appropriate antibody, anti-Lm (C and D, lanes 3 and 7; E and F, lanes 3 and 6), anti-Fn (C and D, lanes 4 and 8; E and F, lanes 4 and 7), anti-Plg (C and D, lanes 5 and 9; E and F, lanes 5 and 8), or anti-pp*Tv*CP4r (C and D, lanes 6 and 10) (1:500 dilution). The positive controls (+) were incubated with an anti-*Tv*TIMr, anti-*Tv*ENOr, or anti-pp*Tv*CP4r antibody, accordingly (lane 2). The controls stained with Coomassie brilliant blue are shown in lane 1. The recombinant *Tv*ENO protein (TVAG_32460) was used as a specific positive control for the interaction with Plg (E, lane 8). The negative controls were obtained by incubating the unrelated recombinant protein pp*Tv*CP4r (F) with Lm (lane 6), Fn (lane 7), and Plg (lane 8) and the corresponding antibodies. Additional negative controls (C and D, lanes 3 to 6; E and F, lanes 3 to 5) were obtained by directly incubating the recombinant proteins tested with the different antibodies used. The protein bands detected by WB were visualized using Quantity One software (Bio-Rad). These experiments were performed at least three independent times, with similar results.

antibodies, accordingly. Figure 5 shows the concentration-dependent binding of *Tv*TIM1r and *Tv*TIM2r to Lm and Fn, as corroborated by densitometric analysis of the black spots detected by WB (Fig. 5A and B). The lack of binding to Plg (Fig. 5) was confirmed using twice as much Plg protein (60 μg ml^{-1}), and the binding observed was compared with the positive reaction of *Tv*ENOr used as an additional positive control for Plg binding, as corroborated by densitometric analysis of the black spots detected by WB (Fig. 5C) with the anti-Plg antibody. Moreover, to assess nonspecific binding, *Tv*CP4r, an unrelated protein, was incubated in increasing amounts (0 to 4 μg) with the three target proteins (Lm, Fn, and Plg) and the corresponding antibodies (anti-Lm, anti-Fn, and anti-Plg). The results showed that none of the three proteins bound to *Tv*CP4r by dot blot binding assays (Fig. 5D). All together, these data demonstrate the ability of both recombinant *Tv*TIM proteins to specifically bind to the Lm and Fn ECM proteins. Thus, our next aim was to determine whether surface-associated *Tv*TIM can help *T. vaginalis* to bind to Lm and Fn under different glucose conditions.

Adherence of *T. vaginalis* to immobilized Lm and Fn is influenced by glucose. To determine the effect of glucose on the adherence of *T. vaginalis* to Lm and Fn, protein binding assays were performed with live parasites. Parasites grown under GR, NG, or HG conditions were labeled with CellTracker Blue (a fluorescent reagent) and added to microtiter wells coated with Lm, Fn, or BSA, used as an unrelated protein and specificity control. Attached parasites were analyzed by optical microscopy (Fig. 6A and B). The images showed that greater numbers of parasites were attached to Lm and Fn when they were grown under NG and HG conditions than under GR conditions; however, the numbers of BSA-attached parasites grown under different glucose concentrations appear to be similar (data not shown). These results were corroborated by quantifying the total fluorescence of the parasites attached to Lm, Fn, and BSA. The bar graphs show the increases in the relative fluorescence units of the parasites attached to Lm (Fig. 6C) and Fn (Fig. 6D), according to the glucose condition, but no increase was observed for BSA, which remained similar (Fig. 6C and D). The highest adherence to Lm and Fn was observed for the parasites grown under HG conditions. These differences in adherence were significant ($P < 0.05$). These data show that glucose promotes the adherence of *T. vaginalis* to Lm and Fn.

Anti-*Tv*TIM antibody inhibits the binding of *T. vaginalis* to Lm and Fn. To demonstrate the role of the surface-associated *Tv*TIM protein in the attachment of *T. vaginalis* to Lm and Fn, adherence inhibition assays using an anti-*Tv*TIMr antibody were performed. As shown in Fig. 2A and 6, the surface localization of *Tv*TIM and the maximum binding of live parasites to Lm and Fn occurred at the highest glucose concentration. Therefore, parasites under HG conditions that had been previously labeled with CellTracker Blue were incubated with increased concentrations (0 to 400 μg ml^{-1}) of anti-*Tv*TIMr IgGs before being added to microtiter wells coated with Lm and Fn. IgGs from PI rabbit serum and an unrelated anti-pp*Tv*CP4r antibody were used as negative controls. After 30 min of interaction of the parasites with Lm and Fn, the fluorescence emission at 466 nm from attached parasites was quantified and compared with the values obtained for the attachment to Lm- or Fn-coated wells of parasites without any treatment (0 μg ml^{-1} of IgG), which was taken as a 100% adherence to ECM proteins. Figure 7A and B show that the anti-*Tv*TIMr antibody specifically inhibited the binding of *T. vaginalis* to im-
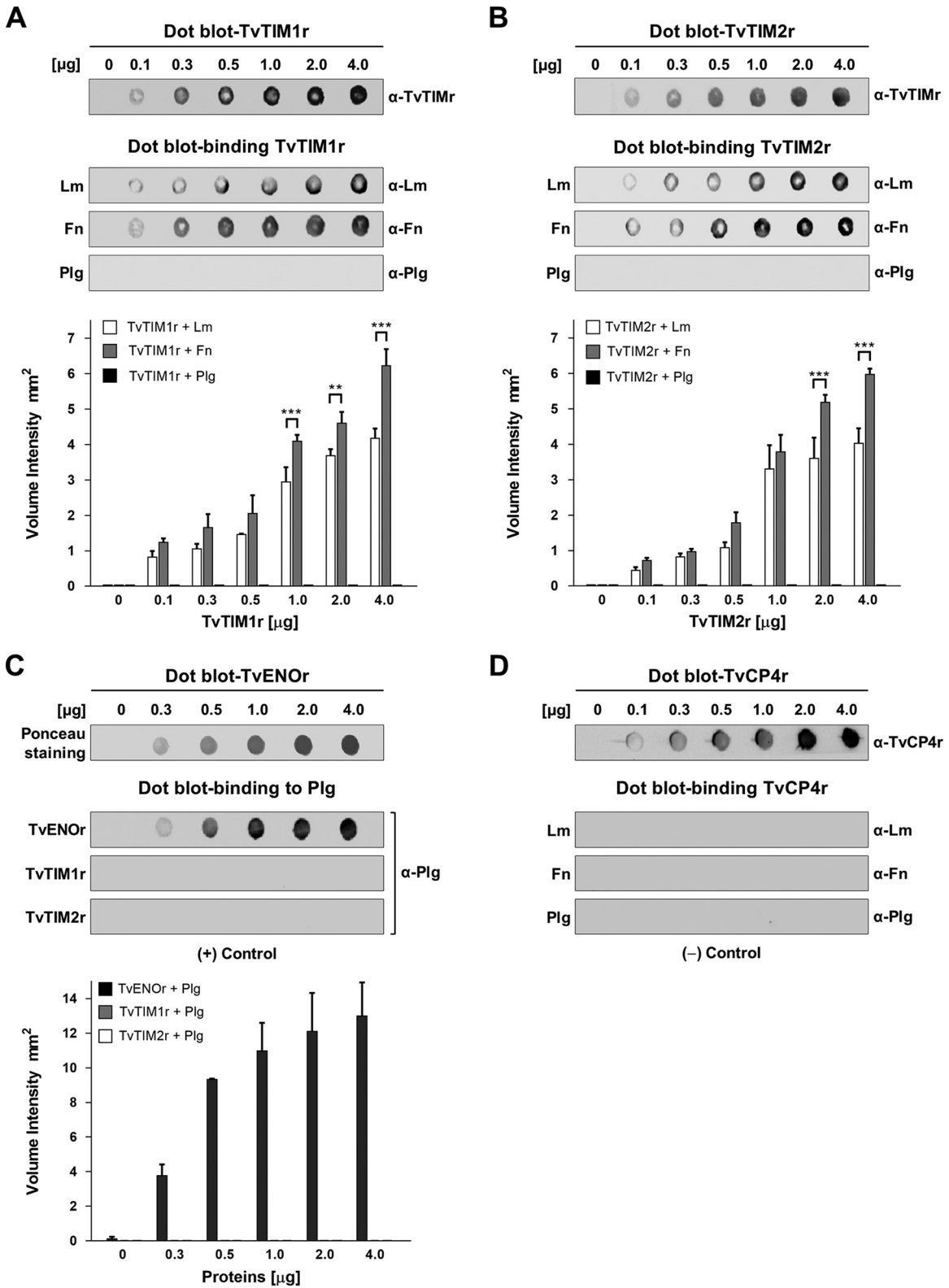
FIG 5 Dot blot-binding assay confirmed the interaction of Lm and Fn with the recombinant *Tv*TIM proteins of *T. vaginalis*. (A and B) For dot blot binding assays, increasing amounts (0 to 4 μg) of *Tv*TIM1r and *Tv*TIM2r were immobilized onto NC membranes and incubated with Lm, Fn, or Plg (30 μg ml^{-1}). The binding of Lm, Fn, and Plg to *Tv*TIM1r or *Tv*TIM2r was detected by WB using an anti-Lm, anti-Fn, or anti-Plg antibody, respectively, followed by a peroxidase-conjugated secondary antibody. The intensities of the black spots indicate positive interactions in relation to the amount of immobilized protein. (C) Different amounts (0 to 4 μg) of *Tv*ENOr (positive control), *Tv*TIM1r, and *Tv*TIM2r were immobilized onto NC membranes and incubated with 30 μg ml^{-1} of Plg for *Tv*ENOr or 60 μg ml^{-1} of Plg for *Tv*TIM1r and *Tv*TIM2r. The specific protein-protein interactions were detected by WB using an anti-Plg antibody, and positive
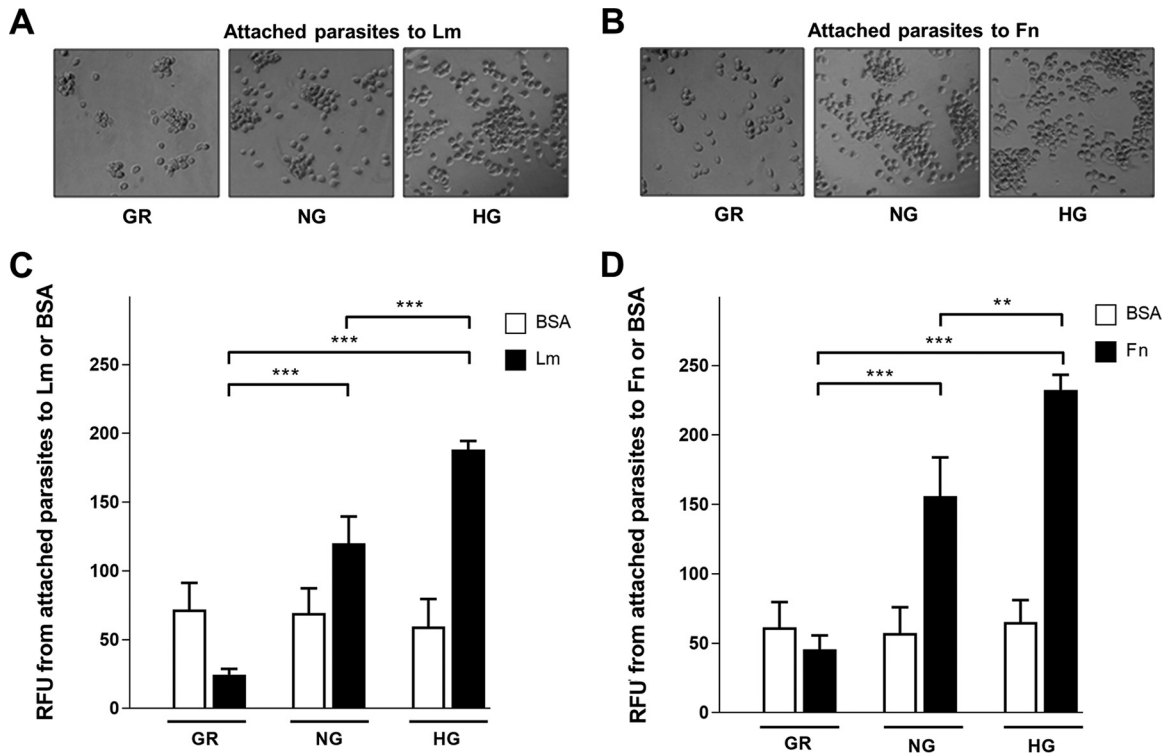
FIG 6 Glucose promotes the adherence of *T. vaginalis* to Lm and Fn. For adherence assays, live parasites (5×10^5 cells per well) grown under GR, NG, or HG conditions were labeled with CellTracker Blue (CTB), added to microtiter wells coated with Lm or Fn (2 μg), and incubated for 30 min at 37°C. The light microscopy images show the attachment of the parasites to Lm (A) and Fn (B) under the different glucose conditions. The number of bound parasites was estimated indirectly by measuring the fluorescence at 466 nm using a Gemini EM spectrofluorometer. The bar graphs show the relative fluorescence units (RFUs) of the parasites attached to Lm (C) or Fn (D) under each glucose condition. The negative specificity controls were obtained using parasites attached to BSA-coated wells under each glucose condition. The error bars indicate the SDs determined from three independent experiments performed in triplicate wells for each condition. The asterisks (** and ***) show the significant differences ($P < 0.05$) among the attached parasites under the three glucose conditions, as determined by ANOVA.

mobilized Lm and Fn in a concentration-dependent manner. No similar inhibition was observed with the anti-pp*Tv*CP4r or PI serum IgGs. In both cases, 400 μg ml^{-1} of anti-*Tv*TIMr IgGs resulted in the maximal inhibition of *T. vaginalis* adherence to Lm and Fn (43.8% and 53.5% inhibition, respectively), indicating that the anti-*Tv*TIMr antibody specifically blocked the binding of the *Tv*TIM proteins on the trichomonad surface to these ECM proteins.

_Tv_TIM recombinant proteins also inhibit _T. vaginalis_ binding to Lm and Fn. To confirm the abilities of *Tv*TIM proteins associated with the surface of *T. vaginalis* to bind to Lm and Fn, competition assays were also performed using purified recombinant *Tv*TIM proteins. To this end, 96-well plates coated with Lm and Fn were preincubated with increasing amounts (0, 0.1, 0.2, 0.4, 0.8, and 1.6 μg) of *Tv*TIM1r or *Tv*TIM2r before interaction with live parasites. Similar increasing amounts of pp*Tv*CP4r were

used as negative controls. Parasites grown under HG conditions that had been previously labeled with CellTracker Blue were added to the protein-coated wells, and the fluorescence emission from the attached parasites was quantified and compared with the values obtained from the attachment of parasites to Lm- or Fn-coated wells without any treatment, which was taken as a 100% adherence to ECM proteins. Figure 7 also shows that *Tv*TIM1r (Fig. 7C) and *Tv*TIM2r (Fig. 7D) blocked the binding of *T. vaginalis* to Lm and Fn via concentration-dependent ligand competition, while no competition was observed with pp*Tv*CP4r. Moreover, 1.6 μg of *Tv*TIM1r and *Tv*TIM2r inhibited the binding of *T vaginalis* to Lm by ~39 and 47%, respectively (Fig. 7C) and the binding to Fn by ~47 and 60%, respectively (Fig. 7D). These results are consistent with the inhibition found using the anti-*Tv*TIMr IgGs (Fig. 7A and B), confirming

interactions are shown as black spots. (D) Different amounts (0 to 4 μg) of *Tv*CP4r (an unrelated recombinant protein) were incubated with Lm, Fn, and Plg (30 μg ml^{-1}). The specific protein-protein interactions were detected by WB using the corresponding antibodies. The absence of black spots indicates that *Tv*CP4r did not bind Lm, Fn, or Plg. This assay was used as a negative control for dot blot binding. As an additional positive control, different amounts (0 to 4 μg) of *Tv*TIM1r (A), *Tv*TIM2r (B), and *Tv*CP4r (D) were directly incubated with anti-*Tv*TIMr or anti-*Tv*CP4r antibody, respectively, followed by a peroxidase-conjugated secondary antibody. The bar graphs show densitometric analysis results for each spot as volume intensity per square millimeter, as determined using Quantity One software (Bio-Rad). The error bars indicate the SDs determined from three independent experiments. For the dot blot positive control, increasing concentrations of *Tv*TIM1r and *Tv*TIM2r were incubated with an anti-*Tv*TIMr antibody, followed by a peroxidase-conjugated secondary antibody. The asterisks (** and ***) show significant differences ($P < 0.05$) among the spots detected by WB, as determined by ANOVA.
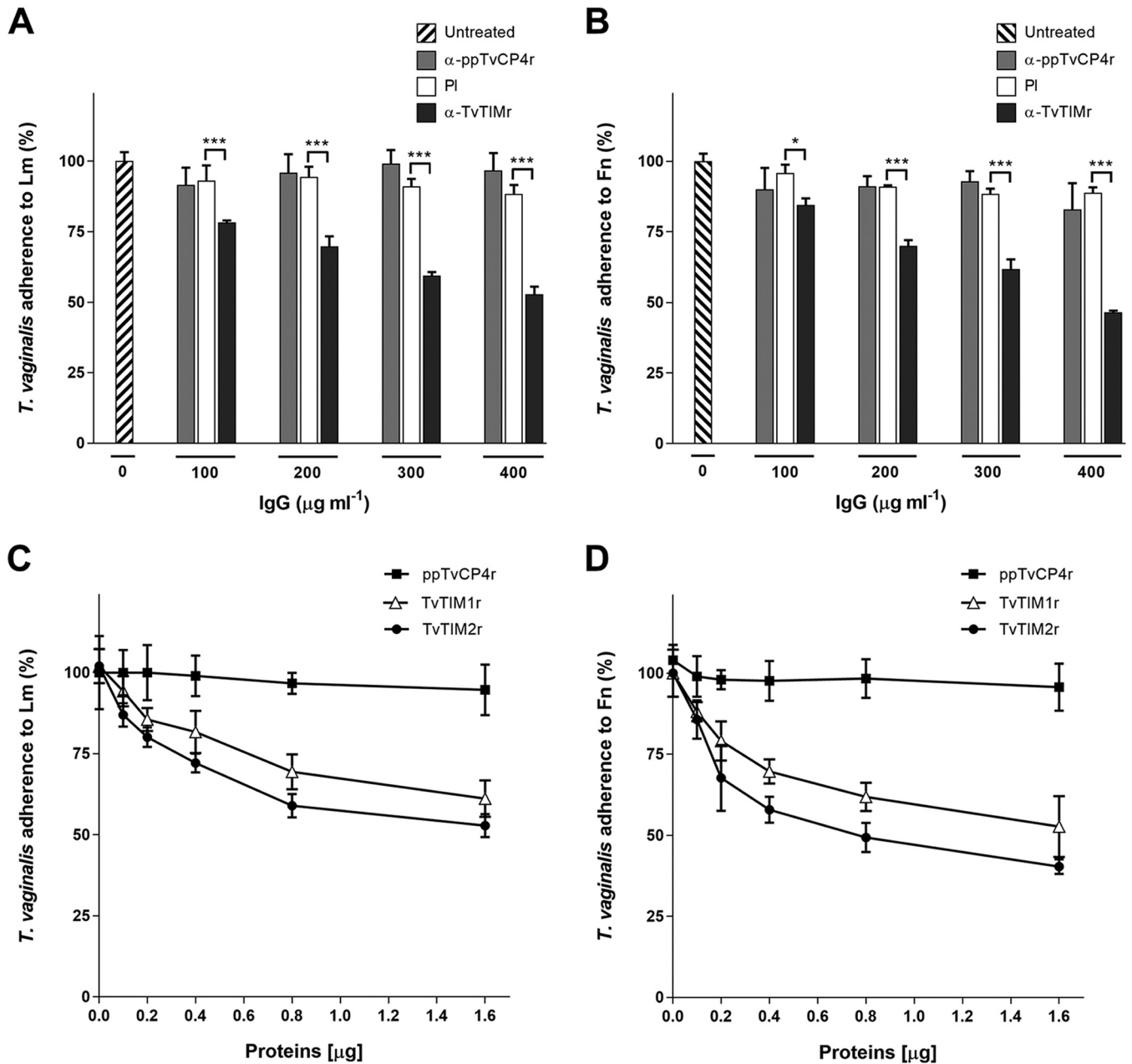
FIG 7 *Tv*TIM on the parasite surface mediates the specific binding of *T. vaginalis* to Lm and Fn, under HG conditions. (A and B) For inhibition assays performed using an anti-*Tv*TIMr antibody, parasites grown in HG (5×10^5 cell ml^{-1}) that had been previously labeled with CellTracker Blue (CTB) were incubated with increasing concentrations (0 to 400 μg ml^{-1}) of anti-pp*Tv*CP4r IgGs before interaction with immobilized Lm (A) or Fn (B) for 30 min at 37°C. The fluorescence emission at 466 nm from the attached parasites was quantified using a Gemini EM spectrofluorometer. The direct binding of untreated CTB-labeled parasites to Lm- or Fn-coated wells (with absolute values of 171.74 and 209.48 RFU, respectively) was taken as 100% binding. IgGs from the PI serum and an unrelated anti-pp*Tv*CP4r antibody were used as negative controls. The bar graphs show the mean percentages of adherence obtained from three independent experiments using triplicate samples. The error bars indicate the SDs, and the asterisks (* and ***) show the significant differences ($P < 0.05$) as determined by ANOVA. (C and D) For competition assays using the recombinant *Tv*TIM proteins as competitors, the Lm- or Fn-coated wells were preincubated with increasing amounts (0 to 1.6 μg per well) of *Tv*TIM1r, *Tv*TIM2r, or pp*Tv*CP4r as a negative control, before interaction for 30 min at 37°C with live parasites grown under HG conditions and labeled with CTB. Finally, the fluorescence emission from the attached parasites at 466 nm was quantified using a Gemini EM spectrofluorometer. The direct binding of CTB-labeled parasites to Lm- or Fn-coated wells in the absence of competitors (with absolute values of 171.74 and 209.48 RFU, respectively) was taken as 100% binding. Each point represents the mean percentage of attached parasites in the presence of a competitor (*Tv*TIM1r, *Tv*TIM2r, or pp*Tv*CP4r). The error bars indicate the SDs from three independent experiments performed in triplicate wells for each condition.

the additional role of *Tv*TIM proteins in Lm and Fn binding of *T. vaginalis*.

T. vaginalis is exposed to different glucose concentrations during vaginal infection. To determine the glucose concentration

that *T. vaginalis* could be exposed to during infection, we measured the amount of glucose present in vaginal secretions of 85 Mexican women that had either healthy vaginal microbiotas or vaginal infections by *T. vaginalis* or by other pathogens. Table 1

TABLE 1 Summary of glucose levels in vaginal secretions of women with healthy vaginal microbiotas and vaginal infections

Sample no.	Age of subject (yrs)	pH	Clinical diagnosis	Microscopic analysis[a]					In vitro culture[c]	Glucose (mM)[d]
				VECs[b]	WBCs	Bacteria	Yeasts	*T. vaginalis*		
Normal microbiotas										
1	37	4	Ovarian cyst	+	+	+ +	−	−	NPI	0.3
2	38	8	Uterine myomatosis	+	+	+	−	−	NPI	0.55
3	42	5	Cystocele	+	+	+	−	−	NPI	0.55
4	33	4	Pregnancy	+ +	+	+	−	−	NPI	0.55
5	31	5	Urinary tract infection, cervicovaginitis	+ +	+ +	+ +	−	−	NPI	2.2
6	24	4	Cervicovaginitis, pregnancy	+	+	+	−	−	NPI	2.2
7	35	7	Cervicovaginitis, ovarian dysfunction	+	+	+	−	−	NPI	2.8
8	54	7	Uterine myomatosis	+	+	+	−	−	NPI	2.8
9	65	7	Cystocele	+ +	+ +	+ +	−	−	NPI	3.05
10	36	5	Dysmenorrhea	+	+ + +	+ + +	−	−	NPI	3.9
11	60	7	Cysteceles	+	+ + +	+ + +	−	−	NPI	3.9
12	24	4	Painful intercourse	+ +	+ +	+	−	−	NPI	7.5
13	33	4	Urinary tract infection, infertility	+ +	+	+ +	−	−	NPI	18.3
14	30	4	Pregnancy	+ + +	+	+ +	−	−	NPI	21.65
15	40	4	Uterine myomatosis	+ + +	+ +	+ +	−	−	NPI	23.05
16	29	5	Urinary tract infection	+ +	+ +	+ +	−	−	NPI	25.25
17	38	7	Chronic vaginitis, polycystic ovary	+ +	+	+ + +	−	−	NPI	25.8
18	37	4	Ovarian cyst	+ +	+	+ + +	−	−	NPI	26.35
19	37	4	Chronic vulvovaginitis	+	+	+	−	−	NPI	30.25
20	45	6	Cystocele	+	+	+	−	−	NPI	38.3
Trichomonas vaginalis										
21	25	4	Cervicovaginitis	+ +	+ +	+ +	−	−	*T. vaginalis* (−)*	0.3
22	26	4	Cervicovaginitis	+ +	+	+ +	−	−	*T. vaginalis* (−)*	0.3
23	43	5	Cervicovaginitis	+ +	+ +	+ +	−	−	*T. vaginalis* (−)*	0.3
24	44	6	Cervicovaginitis	+ + +	+ + +	+ +	−	−	*T. vaginalis* (−)*	0.3
25	50	5	Cervicovaginitis	+	+	+	−	−	*T. vaginalis* (−)*	0.3
26	65	7	Cervicovaginitis	+	+	+	−	−	*T. vaginalis* (−)*	0.3
27	23	6	Cervicovaginitis	+	+	+	−	−	*T. vaginalis* (−)*	0.55
28	33	5	Cervicovaginitis	+ +	+ +	+ +	−	−	*T. vaginalis* (−)*	0.55
29	38	4	Cervicovaginitis	+	+ + +	+ +	−	−	*T. vaginalis* (−)*	0.55
30	42	5	Cervicovaginitis	+	+	+	−	−	*T. vaginalis* (−)*	0.55
31	25	6	Cervicovaginitis	+ + +	+ + +	+ + +	−	−	*T. vaginalis* (−)*	0.85
32	42	7	Cervicovaginitis	+ +	+ +	+	−	−	*T. vaginalis* (−)*	0.85
33	23	5	Cervicovaginitis	+	+	+	−	−	*T. vaginalis* (−)*	1.95
34	29	6	Cervicovaginitis	+	+	+	+	−	*T. vaginalis* (−)*	1.95
35	29	6	Cervicovaginitis	+ +	+ +	+ + +	−	−	*T. vaginalis* (−)*	2.2
36	27	4	Cervicovaginitis	+ + +	+ +	+ +	+	−	*T. vaginalis* (−)*	2.2
37	44	5	Cervicovaginitis	+ +	+ +	+ + +	+	−	*T. vaginalis* (−)*	2.5
38	42	5	Cervicovaginitis	+ +	+ +	+	−	−	*T. vaginalis* (−)*	3.05
39	20	5	Cervicovaginitis	+ +	+ +	+ +	−	−	*T. vaginalis* (−)*	3.35
40	58	6	Cervicovaginitis	+ +	+ +	+ +	−	−	*T. vaginalis* (−)*	3.6
41	33	5	Cervicovaginitis	+	+	+ +	−	−	*T. vaginalis* (−)*	3.9
42	43	4	Cervicovaginitis	+ +	+	+ + +	−	−	*T. vaginalis* (−)*	17.2
43	25	5	Cervicovaginitis	+	+ +	+ +	−	−	*T. vaginalis* (−)*	22.2
44	50	5	Cervicovaginitis	+ +	+	+ +	−	−	*T. vaginalis* (−)*	22.75
45	34	6	Cervicovaginitis	+ +	+	+ + +	−	−	*T. vaginalis* (−)*	25.8
46	29	5	Cervicovaginitis	+ +	+ +	+ +	−	−	*T. vaginalis* (−)*	26.9
47	50	4	Cervicovaginitis	+ +	+ +	+ +	+	−	*T. vaginalis* (−)*	28.3
48	20	5	Cervicovaginitis	+ +	+	+	−	−	*T. vaginalis* (−)*	28.3
49	31	5	Cervicovaginitis	+ +	+	+ +	−	−	*T. vaginalis* (−)*	30.55
50	59	5	Cervicovaginitis	+ +	+	+	−	−	*T. vaginalis* (−)*	31.1
51	36	6	Cervicovaginitis	+ +	+ +	+ +	−	−	*T. vaginalis* (−)*	31.35
52	52	5	Cervicovaginitis	+ +	+ +	+ + +	−	−	*T. vaginalis* (−)*	31.66
53	37	5	Cervicovaginitis	+ +	+	+ +	+ +	−	*T. vaginalis* (−)*	36.1
54	47	4	Cervicovaginitis	+ +	+ +	+ + +	−	−	*T. vaginalis* (−)*	39.15
55	26	5	Cervicovaginitis	+ +	+ +	+ +	−	−	*T. vaginalis* (−)*	42.2

(Continued on following page)

TABLE 1 (Continued)

Sample no.	Age of subject (yrs)	pH	Clinical diagnosis	Microscopic analysis[a]					In vitro culture[c]	Glucose (mM)[d]
				VECs[b]	WBCs	Bacteria	Yeasts	T. vaginalis		
56	24	6	Cervicovaginitis	+++	++	++	−	−	T. vaginalis (−)*	42.45
57	41	4	Cervicovaginitis	++	++	+++	−	−	T. vaginalis (−)*	43.1
Trichomonas vaginalis										
58	33	5	Cervicovaginitis	+	+	++	−	+	T. vaginalis (+)*	0.3
59	52	5	Cervicovaginitis	++	++	+++	−	+	T. vaginalis (+)*	0.3
60	26	6	Cervicovaginitis	++	++	++	+	+	T. vaginalis (+)*	0.3
61	40	5	Cervicovaginitis	++	+	+++	−	+	T. vaginalis (+)*	0.85
62	35	5	Cervicovaginitis	++	++	+++	−	+	T. vaginalis (+)*	0.85
63	25	6	Cervicovaginitis	+++	++	++	−	+	T. vaginalis (+)*	1.1
64	19	5	Cervicovaginitis	+++	++	+++	−	+	T. vaginalis (+)*	1.1
65	40	5	Cervicovaginitis	+	+	+++	−	+	T. vaginalis (+)*	1.65
66	44	5	Cervicovaginitis	+++	+	+++	−	+	T. vaginalis (+)*	1.65
67	40	6	Cervicovaginitis	+	+	+	−	+	T. vaginalis (+)*	2.2
68	42	5	Cervicovaginitis	++	++	+++	−	+	T. vaginalis (+)*	19.45
69	61	6	Cervicovaginitis	++	++	++	−	+	T. vaginalis (+)*	25.25
70	42	5	Cervicovaginitis	++	++	+	−	+	T. vaginalis (+)*	30.8
71	35	5	Cervicovaginitis	++	+	++	−	+	T. vaginalis (+)*	31.35
72	20	5	Cervicovaginitis	+	+	++	+	+	T. vaginalis (+)*	36.65
Other pathogens										
73	25	6	Cervicovaginitis	++	+++	++	−	−	G. vaginalis	0.55
74	19	5	Cervicovaginitis	++	+	++	−	−	G. vaginalis	1.1
75	29	5	Hypothyroidism	+++	++	+++	−	−	G. vaginalis	1.95
76	29	4	Human papillomavirus	++	+	+	−	−	C. albicans	1.4
77	47	5	Urosepsis	+++	+	++	−	−	C. albicans	2.2
78	26	4	Pregnancy	+	+	+	−	−	C. albicans	2.2
79	21	5	Cervicovaginitis, pregnancy	+++	+++	+++	−	−	C. albicans	2.5
80	27	5	Cervicovaginitis	++	++	++	−	−	C. albicans	4.45
81	24	7	Cervical cancer	+	+	+	−	−	C. albicans	25.25
82	47	4	Cervicovaginitis	++	++	++	+++	−	C. albicans	41.35
83	34	5	Urinary tract infection, infertility	+	+	+	−	−	Enterobacteria	3.9
84	58	7	Urinary tract infection, cervicovaginitis	++	++	++	−	−	Enterobacteria	31.9
85	66	7	Diabetes mellitus type 2	+	+	+	−	−	Enterobacteria	56.6

[a] Signs show the abundance of cellular components as follows: +, few; ++, moderate; +++, abundant; −, absent.
[b] VEC, vaginal epithelial cells.
[c] In vitro culture was performed for isolation of bacteria, fungi, or *T. vaginalis*. NPI, no pathogen isolated by culture; however, culture for the isolation of *T. vaginalis* was not performed. An asterisk indicates that only the *in vitro* culture for isolation of *T. vaginalis* was performed.
[d] Glucose levels in vaginal secretions were determined by the automatic hexokinase method.

shows the individual values of the vaginal glucose concentration for each person tested. For the group of women with healthy vaginal microbiotas but with gynecological problems, the average glucose concentration in vaginal secretions was 11.96 mM; however, individual values varied between 0.3 and 38.3 mM. For the group of women with cervicovaginitis but without *T. vaginalis* infection, the average glucose concentration was 14.31 mM, with individual values that varied between 0.3 and 43.1 mM. For the group of women with *T. vaginalis* infection, the average glucose concentration was 10.25 mM, with individual values that varied between 0.3 and 36.65 mM. In women with vaginal infection by other pathogens, such as *Candida albicans*, *Gardnerella vaginalis*, and enterobacteria, the average glucose concentration was 13.48 mM, with individual values between 0.55 and 56.6 mM. These data show that the glucose levels in vaginal secretions of the three groups of women included in this study were variable. These data suggest that *T. vaginalis* could be exposed to varied vaginal glucose

concentrations during infection. These changes in vaginal glucose could modulate the interaction of *T. vaginalis* with extracellular matrix components. It is important to mention that the glucose levels reported in this study are subject to different variables, such as age, pH, and clinical diagnosis.

DISCUSSION

Glycolysis is a critical process for *T. vaginalis* under glucose-rich conditions and is considered an optimal metabolic condition for cell division and establishment of vaginal infection (26). However, under metabolic stress by glucose restriction, *T. vaginalis* activates several adaptive mechanisms, such as metabolic reprogramming, enhancing antioxidant ability, and autophagy, for cellular homeostasis that promotes cell survival (26). These data suggest that *T. vaginalis* has a high capacity to adapt to glucose fluctuations in the environment. Moreover, glucose levels modulate the expression

and specific activity of enzymes involved in the glucose metabolism of *T. vaginalis* (26, 34).

Interestingly, the majority of these metabolic enzymes are encoded by one or more gene copies in the *T. vaginalis* genome (35). In other organisms, gene duplication is the primary source of new genes with expression divergence and protein subcellular relocalization, and gene duplication is also related to the acquisition of new functions (36, 37). Similar mechanisms have been associated with the emergence of alternative novel functions in glycolytic enzymes localized on the surface of *T. vaginalis*, where they exhibit new functions as adhesins or receptor molecules for ECM components, in addition to their cytoplasmic metabolic functions (6). This dual function has led to their classification as "moonlighting proteins" that can switch between functions following changes in cellular localization, or following modulation by alterations in the concentrations of certain environmental components (38, 39), by posttranslational modifications, or even by a single amino acid mutation that can result in the creation of a new function (39). For example, some glycolytic enzymes that are localized on the surface of *T. vaginalis* exhibit new functions as adhesins (6, 8, 9, 29) or receptor molecules for ECM components, participating in host-parasite interactions (11, 12). However, this topic has been controversial for the trichomonad community (4, 40–42), because like other moonlighting proteins (14, 39), these molecules lack TMDs and SPs; the pathway used by the proteins to reach the parasite membrane is still unknown (14, 39), and their receptors have not been identified yet. In this study, we demonstrated that glucose differentially regulates the expression of the two *Tv*TIM-encoding genes (Fig. 1B) and induces the expression and surface localization of *Tv*TIM (Fig. 1C, 2, and 3). Furthermore, surface-associated *Tv*TIM mediates specific binding to Lm and Fn under HG conditions (Fig. 4 to 7), which provides an additional role for *Tv*TIM in the adherence of *T. vaginalis* to the host ECM proteins Fn and Lm.

*Tv*TIM is encoded by two genes (*tvtim1* and *tvtim2*) (23), a feature associated with expression divergence in other organisms (36, 37). Although the nucleotide sequences of the two *tvtim* genes are 97.6% identical, our results showed that they were differentially expressed in response to glucose (*tvtim1* was negatively regulated, whereas *tvtim2* was positively regulated) (Fig. 1B). These results are consistent with transcriptomic studies revealing the overexpression of *tvtim2*, but not *tvtim1*, in parasites grown under HG conditions (26) and in contact with vaginal epithelial cells (42) or with Fn (25). These data suggest that the transcription of the *tvtim* genes is differentially regulated during *in vitro* infection, in contact with ECM proteins such as Fn, and by glucose via still-unknown regulatory elements that control the expression of each gene, resulting in different functions and localizations. A similar mechanism has been proposed for yeasts that have regulatory motifs that diverge between duplicated genes and that are related to the protein evolution for new functions (43).

We also showed that *Tv*TIM was modulated by the glucose concentration at the protein level (Fig. 1C). The amino acid sequences of the two *Tv*TIM proteins are 98.4% identical, differing by only four amino acids but showing remarkable differences in physicochemical properties, dimer stability, and enzymatic activity (23, 24, 44). Thus, it was impossible to differentiate between *Tv*TIM1 and *Tv*TIM2 using an anti-*Tv*TIMr antibody. However, when we take into account the opposite effects of glucose on *tvtim* gene expression (Fig. 1B), our data suggest that the increase in the

amount of *Tv*TIM protein in parasites grown under HG conditions could correspond to the *Tv*TIM2 protein. This hypothesis is consistent with the results of the proteomics analysis of exosomes (45): *Tv*TIM2, but not *Tv*TIM1, has been found to be associated with the exosomal proteins of *T. vaginalis* (45), suggesting that *Tv*TIM2 is among the proteins secreted through an unconventional vesicular pathway (46). Consistent with this unconventional trafficking pathway, *Tv*TIM gold label was observed in multivesicular body (MVB)-like structures fused with the parasite membrane (Fig. 3A, panel g) that may correspond to *Tv*TIM2. Thus, in the near future, investigations should be conducted to determine whether only one or both *Tv*TIM proteins are localized to the surface of *T. vaginalis* to acquire moonlighting functions as an Lm- and Fn-binding protein under HG conditions and whether one or both proteins are part of the secretome.

We also found that hexokinase (*Tv*HK) was positively modulated by glucose, whereas alpha-enolase (*Tv*ENO) and malic enzyme/AP65 were not affected (Fig. 1C). These data show that glucose levels regulate the amount of glycolytic enzymes of the first reactions in the glycolytic pathway in *T. vaginalis* (7, 26, 35). The behavior of the *Tv*TIM proteins of *T. vaginalis* is similar to that observed in the TIM protein of *Fusobacterium varium*, which specifically increases in response to the presence of environmental glucose (47), supporting the positive regulation of TIM by glucose also observed in *T. vaginalis*.

In addition to the expected cytoplasmic localization, *Tv*TIM also showed a second localization to the surface of *T. vaginalis* parasites grown under HG conditions (Fig. 2), moonlighting with a novel function as an Lm and Fn receptor that supports the interaction of *T. vaginalis* with these ECM proteins (48), similar to that observed in other organisms (14, 38). This behavior is similar to that of other trichomonad glycolytic enzymes, *Tv*GAPDH and *Tv*ENO, with alternative surface localizations in response to iron exposure and cellular contact with VECs, respectively (11, 12). Interestingly, all these glycolytic enzymes have also been found to be associated with the surface of *Entamoeba histolytica* (49) and the cell wall of *C. albicans* (50) to perform new functions in the host-parasite interplay. Therefore, here we have shown that glucose is another environmental factor that differentially regulates gene expression as well as the amount and surface localization of glycolytic enzymes in *T. vaginalis*.

The mechanism by which *Tv*TIM reaches the surface of *T. vaginalis* under different environmental conditions is unclear because this enzyme does not have a TMD or an SP like most of the reported moonlighting proteins (14, 39). However, alternative, unconventional trafficking pathways for its relocalization to the parasite surface have been proposed, for example, through secretory vesicles, such as exosomes, which are intracellularly derived from multivesicular bodies and are released when they fuse with the plasma membrane (46). Our data from immunogold TEM experiments evaluating the localization of *Tv*TIM (Fig. 3A) support the presence of unconventional secretory pathways involved in *Tv*TIM trafficking from cytoplasm to the plasma membrane, mainly through secretory vesicles. However, a pathway independent of vesicles is also evident (Fig. 3). Interestingly, we found that *Tv*TIM also attached to the internal and external faces of vesicles near the membrane, like the *Tv*Gα402 localization previously described (51), which may also be involved in some of the trichomonad trafficking pathways and in vesicles that fused with the plasma membrane. Moreover, after fusion with the plasma

membrane, *Tv*TIM is also exposed to the external surface of the cells (Fig. 3). Similar mechanisms have been identified for other glycolytic enzymes associated with secretory vesicles, such as exosomes or shedding vesicles (52). Interestingly, *Tv*TIM2, but not *Tv*TIM1, has been found to be associated with the exosomal proteins of *T. vaginalis* (45), suggesting that *Tv*TIM2 could be the protein with alternate functions localizing to the surface of *T. vaginalis*, behaving as another intracellular glycolytic enzyme that moonlights to the parasite surface (52, 53), acquiring a new function as an Lm and Fn receptor (48). Therefore, the presence of *Tv*TIM in MVBs and secretory vesicles (Fig. 3) suggests the involvement of an unconventional vesicular trafficking pathway for *Tv*TIM and possibly for other surface-associated glycolytic enzymes in *T. vaginalis*. It will be interesting to investigate whether G proteins also found in MVB-like compartments and secretory vesicles, like *Tv*Gα402 (51), can participate in the trafficking pathway for surface-associated *Tv*TIM.

The possibility that the affinity of *T. vaginalis* *Tv*TIM for lipid membranes could be related to cotranslational or posttranslational modifications (PTMs) is also a plausible hypothesis that has to be tested. In support of this hypothesis, *in silico* analysis of *Tv*TIM sequences shows that both *Tv*TIM proteins contain putative sites for S-palmitoylation (cluster C) and N-myristoylation; both modifications could be involved in the interaction of the proteins with lipid membranes (54–56). Additionally, we identified putative sites for phosphorylation (on S and T), which may be important for interactions with other proteins or substrates and N- or O-glycosylation and thus could be relevant for protein secretion (39). This is interesting and motivates us to confirm these modifications in future experiments to determine their contribution to surface localization and the moonlighting functions of *Tv*TIM and other glycolytic enzymes in *T. vaginalis*. Other studies have shown that some glycolytic proteins are indirectly associated with the extracellular surface. These proteins can interact either with the lipid membrane or with integral membrane proteins through a combination of noncovalent interactions, including hydrophobic and electrostatic interactions (49, 57). A typical example of glycolytic proteins indirectly associated with the surface are the GAPDH and TIM proteins of *Lactobacillus plantarum*, which are noncovalently attached to its outer cell wall (57).

The results of inhibition and competition assays testing the adherence of live parasites to Lm and Fn using antibodies to *Tv*TIMr and both recombinant *Tv*TIM proteins (Fig. 6 and 7) confirm the participation of the surface-associated *Tv*TIM as a new receptor for Lm and Fn that is used by trichomonads to interact with these ECM proteins, extending the results of previous studies (48). Further studies will be necessary to identify and characterize the binding sites of TvTIM for Lm and Fn.

These results are consistent with some of the functions identified for TIM on the surfaces of other pathogens (14, 53), such as *P. brasiliensis* (16) *S. aureus* (17), *L. plantarum* (57), and *Mycoplasma gallisepticum* (58). Recently, the TIM protein was also identified in the surface proteome of *E. histolytica* (49) and in the cell wall proteome of *C. albicans* (50); however, the specific surface function of TIM in *E. histolytica* has not been described yet. Similar strategies have been used to determine the proteome of *T. vaginalis* surface; however, *Tv*TIM proteins were not identified (59).

Our *in vitro* results show that glucose is an important nutrient for the biology of *T. vaginalis*; however, it was unknown whether *T. vaginalis* is exposed to changes in glucose levels during infec-

tion. For this reason, in this study, we also determined the glucose concentration in vaginal secretions from Mexican women with trichomoniasis and other infections (Table 1). We found that the median level of free glucose was 10.25 mM, with individual values between 0.3 and 36.65 mM. Our results are in the range of those recently reported (60). Compared to the highest value of glucose detected in vaginal secretions (36.65 mM) of patients with trichomoniasis, 50 mM glucose, used *in vitro* as the HG condition, was not found in these samples. However, as shown in Fig. 2B, trichomonad parasites are able to respond in the presence of exogenous glucose in the medium that promotes the relocalization of *Tv*TIM to the plasma membrane, confirmed by the colocalization coefficient, which increased more than 2-fold at 10 and 25 mM glucose and about 3-fold at 50 mM glucose. Although the colocalization of *Tv*TIM on the parasites surface at 50 mM glucose could appear low (Fig. 2B) compared with those shown in Fig. 2A, we have to consider that the times of exposures to glucose were different, 1 h and 24 h, respectively. Even if in our study, we used the maximum glucose concentrations previously reported (26) for purposes of comparison between GR and HG conditions, our data (Fig. 2B) show that the vaginal glucose concentrations found in at least 67% of women with *T. vaginalis* (Table 1) can trigger the relocalization of *Tv*TIM to the parasite surface during infection and to be responsible for the parasite adherence to ECM proteins Lm and Fn, as shown in Fig. 6. In addition, we do not rule out the possibility of the parasite finding glucose concentrations near 50 mM in other infected women, such as those with diabetes mellitus type 2 (56 mM glucose in vaginal secretions) (Table 1). Furthermore, a GR condition (≤1 mM) was found in 33% of samples with trichomoniasis, in 20% of women with healthy vaginal microbiotas but with gynecological problems, in 32% of women with cervicovaginitis but without *T. vaginalis* infections, and in 7% of women with vaginal infections with other pathogens (Table 1). Our results show a large variability in free glucose levels among women included in this study, which is consistent with those previously reported (60), suggesting that *T. vaginalis* could be exposed to glucose fluctuations during infection. Taking into account our results, these changes in vaginal glucose could modulate the interaction of *T. vaginalis* with ECM components *in vivo*. Similarly, *C. albicans* is another pathogen that causes vaginal infection that is responsible for vulvo-vaginal candidiasis. Studies show that this fungal has a high prevalence among women with diabetes mellitus, possibly related to their hyperglycemic status, which promotes the colonization of the vaginal tract in this group (61, 62).

An important question is why parasites need to localize some glycolytic enzymes on their surface. A possible explanation is the adaptive advantages that this mechanism provides to parasites during infection; for example, glycolytic enzymes may act as ligands for a variety of components of the host. This binding would allow the parasites to recognize the host cell for adherence and invasion, modulate hemostatic and immune systems, promote angiogenesis, or acquire molecules for nutrition (52) even as protective molecules for the oxidative burst, as occurs for *C. albicans* (50). For *T. vaginalis*, we can postulate as previously mentioned (11, 12) that the focal sites of erosion in the vaginal epithelium due to parasite proteolytic activity can result in *T. vaginalis* access to ECM and basal membrane proteins, such as Fn and Lm, and the surface-associated *Tv*TIM could then contribute to parasite adherence to ECM proteins, interactions that appear to be required

to maintain a chronic infection by this sexually transmitted parasite (48).

In conclusion, the glucose-induced *Tv*TIM protein is a glycolytic enzyme associated with the surface of *T. vaginalis* with a novel function, participating as a virulence factor in interactions with ECM and basal membrane proteins such as Fn and Lm.

REFERENCES

1. **Poole DN, McClelland RS.** 2013. Global epidemiology of *Trichomonas vaginalis*. Sex Transm Infect **89:**418–422. http://dx.doi.org/10.1136/sextrans-2013-051075.

2. **Lehker MW, Alderete JF.** 2000. Biology of trichomonosis. Curr Opin Infect Dis **13:**37–45. http://dx.doi.org/10.1097/00001432-200002000-00007.

3. **Hirt RP, Sherrard J.** 2015. Trichomonas vaginalis origins, molecular pathobiology and clinical considerations. Curr Opin Infect Dis **28:**72–79. http://dx.doi.org/10.1097/QCO.0000000000000128.

4. **Kusdian G, Gould SB.** 2014. The biology of *Trichomonas vaginalis* in the light of urogenital tract infection. Mol Biochem Parasitol **198:**92–99. http://dx.doi.org/10.1016/j.molbiopara.2015.01.004.

5. **Lehker MW, Sweeney D.** 1999. Trichomonad invasion of the mucous layer requires adhesins, mucinases, and motility. Sex Transm Infect **75:**231–238. http://dx.doi.org/10.1136/sti.75.4.231.

6. **Figueroa-Angulo EE, Rendón-Gandarilla FJ, Puente-Rivera J, Calla-Choque JS, Cárdenas-Guerra RE, Ortega-López J, Quintas-Granados LI, Alvarez-Sánchez ME, Arroyo R.** 2012. The effect of environmental factors on the virulence of *Trichomonas vaginalis*. Microbes Infect **14:**1411–1427. http://dx.doi.org/10.1016/j.micinf.2012.09.004.

7. **Steinbüchel A, Müller M.** 1986. Anaerobic pyruvate metabolism of *Tritrichomonas foetus* and *Trichomonas vaginalis* hydrogenosomes. Mol Biochem Parasitol **20:**57–65. http://dx.doi.org/10.1016/0166-6851(86)90142-8.

8. **Arroyo R, Engbring J, Alderete JF.** 1992. Molecular basis of host epithelial cell recognition by *Trichomonas vaginalis*. Mol Microbiol **6:**853–862. http://dx.doi.org/10.1111/j.1365-2958.1992.tb01536.x.

9. **Moreno-Brito V, Yáñez-Gómez C, Meza-Cervantez P, Avila-González L, Rodríguez MA, Ortega-López J, González-Robles A, Arroyo R.** 2005. A *Trichomonas vaginalis* 120 kDa protein with identity to hydrogenosome pyruvate:ferredoxin oxidoreductase is a surface adhesin induced by iron. Cell Microbiol **7:**245–258. http://dx.doi.org/10.1111/j.1462-5822.2004.00455.x.

10. **Garcia AF, Chang TH, Benchimol M, Klumpp DJ, Lehker MW, Alderete JF.** 2003. Iron and contact with host cells induce expression of adhesins on surface of *Trichomonas vaginalis*. Mol Microbiol **47:**1207–1224. http://dx.doi.org/10.1046/j.1365-2958.2003.03366.x.

11. **Lama A, Kucknoor A, Mundodi V, Alderete JF.** 2009. Glyceraldehyde-3-phosphate dehydrogenase is a surface-associated, fibronectin-binding protein of *Trichomonas vaginalis*. Infect Immun **77:**2703–2711. http://dx.doi.org/10.1128/IAI.00157-09.

12. **Mundodi V, Kucknoor AS, Alderete JF.** 2008. Immunogenic and plasminogen-binding surface-associated alpha-enolase of *Trichomonas vaginalis*. Infect Immun **76:**523–531. http://dx.doi.org/10.1128/IAI.01352-07.

13. **Ginger ML.** 2014. Protein moonlighting in parasitic protists. Biochem Soc Trans **42:**1734–1739. http://dx.doi.org/10.1042/BST20140215.

14. **Amblee V, Jeffery CJ.** 2015. Physical features of intracellular proteins that moonlight on the cell surface. PLoS One **10:**e0130575. http://dx.doi.org/10.1371/journal.pone.0130575.

15. **Wierenga RK, Kapetaniou EG, Venkatesan R.** 2010. Triosephosphate isomerase: a highly evolved biocatalyst. Cell Mol Life **67:**3961–3982. http://dx.doi.org/10.1007/s00018-010-0473-9.

16. **Pereira LA, Báo SN, Barbosa MS, da Silva JL, Felipe MS, de Santana JM, Mendes-Giannini MJ, de Almeida-Soares CM.** 2007. Analysis of the *Paracoccidioides brasiliensis* triosephosphate isomerase suggests the potential for adhesin function. FEMS Yeast Res **7:**1381–1388. http://dx.doi.org/10.1111/j.1567-1364.2007.00292.x.

17. **Furuya H, Ikeda R.** 2011. Interaction of triosephosphate isomerase from *Staphylococcus aureus* with plasminogen. Microbiol Immunol **55:**855–862. http://dx.doi.org/10.1111/j.1348-0421.2011.00392.x.

18. **Hewitson JP, Rückerl D, Harcus Y, Murray J, Webb LM, Babayan SA, Allen JE, Kurniawan A, Maizels RM.** 2014. The secreted triosephosphate isomerase of *Brugia malayi* is required to sustain microfilaria production *in vivo*. PLoS Pathog **10:**e1004133. http://dx.doi.org/10.1371/journal.ppat.1004133.

19. **Cass CL, Johnson JR, Califf LL, Xu T, Hernandez HJ, Stadecker MJ, Yates JR, Williams DL.** 2007. Proteomic analysis of *Schistosoma mansoni* egg secretions. Mol Biochem Parasitol **155:**84–93. http://dx.doi.org/10.1016/j.molbiopara.2007.06.002.

20. **Harn DA, Gu W, Oligino LD, Mitsuyama M, Gebremichael A, Richter D.** 1992. A protective monoclonal antibody specifically recognizes and alters the catalytic activity of *Schistosoma* triosephosphate isomerase. J Immunol **148:**562–567.

21. **Henze K, Schnarrenberger C, Kellermann J, Martin W.** 1994. Chloroplast and cytosolic triosephosphate isomerases from spinach: purification, microsequencing and cDNA cloning of the chloroplast enzyme. Plant Mol Biol **26:**1961–1973. http://dx.doi.org/10.1007/BF00019506.

22. **Poysti NJ, Oresnik IJ.** 2007. Characterization of *Sinorhizobium meliloti* triosephosphate isomerase genes. J Bacteriol **189:**3445–3451. http://dx.doi.org/10.1128/JB.01707-06.

23. **Figueroa-Angulo EE, Estrella-Hernández P, Salgado-Lugo H, Ochoa-Leyva A, Gómez-Puyou A, Campos SS, Montero-Moran G, Ortega-López J, Saab-Rincón G, Arroyo R, Benítez-Cardoza CG, Brieba LG.** 2012. Cellular and biochemical characterization of two closely related triosephosphate isomerases from *Trichomonas vaginalis*. Parasitology **139:**1729–1738. http://dx.doi.org/10.1017/S003118201200114X.

24. **Lara-González S, Estrella-Hernández P, Ochoa-Leyva A, Portillo-Téllez Del Carmen M, Caro-Gómez LA, Figueroa-Angulo EE, Salgado-Lugo H, Miranda-Ozuna JFT, Ortega-López J, Arroyo R, Brieba LG, Benítez-Cardoza CG.** 2014. Structural and thermodynamic folding characterization of triosephosphate isomerases from *Trichomonas vaginalis* reveals the role of destabilizing mutations following gene duplication. Proteins **82:**22–33. http://dx.doi.org/10.1002/prot.24333.

25. **Huang KY, Huang PJ, Ku FM, Lin R, Alderete JF, Tang P.** 2012. Comparative transcriptomic and proteomic analyses of *Trichomonas vaginalis* following adherence to fibronectin. Infect Immun **80:**3900–3911. http://dx.doi.org/10.1128/IAI.00611-12.

26. **Huang KY, Chen YY, Fang YK, Cheng WH, Cheng CC, Chen YC, Wu TE, Ku FM, Chen SC, Lin R, Tang P.** 2014. Adaptive responses to glucose restriction enhance cell survival, antioxidant capability, and autophagy of the protozoan parasite *Trichomonas vaginalis*. Biochim Biophys Acta **1840:**53–64. http://dx.doi.org/10.1016/j.bbagen.2013.08.008.

27. **Diamond LS.** 1957. The establishment of various trichomonads of animals and man in axenic cultures. J Parasitol **43:**488–490.

28. **León-Sicairos CR, León-Félix J, Arroyo R.** 2004. tvcp12: a novel *Trichomonas vaginalis* cathepsin L-like cysteine proteinase-encoding gene. Microbiology **150:**1131–1138. http://dx.doi.org/10.1099/mic.0.26927-0.

29. **Meza-Cervantez P, González-Robles A, Cárdenas-Guerra RE, Ortega-López J, Saavedra E, Pineda E, Arroyo R.** 2011. Pyruvate:ferredoxin oxidoreductase (PFO) is a surface-associated cell-binding protein in *Trichomonas vaginalis* and is involved in trichomonal adherence to host cells. Microbiology **157:**3469–3482. http://dx.doi.org/10.1099/mic.0.053033-0.

30. **Garcia AF, Alderete JF.** 2007. Characterization of the *Trichomonas vagi-*

nalis surface-associated AP65 and binding domain interacting with trichomonads and host cells. BMC Microbiol **7**:116–126. http://dx.doi.org/10.1186/1471-2180-7-116.

31. **Hinners l. Moschner J, Nolte N, Hille-Rehfeld A.** 1999. The orientation of membrane proteins determined *in situ* by immunofluorescence staining. Anal Biochem **276**:1–7. http://dx.doi.org/10.1006/abio.1999.4325.

32. **Cárdenas-Guerra RE, Ortega-López J, Flores-Pucheta CI, Benítez-Cardoza CG, Arroyo R.** 2015. The recombinant prepro region of TvCP4 is an inhibitor of cathepsin L-like cysteine proteinases of *Trichomonas vaginalis* that inhibits trichomonal haemolysis. Int J Biochem Cell Biol **59**:73–83. http://dx.doi.org/10.1016/j.biocel.2014.12.001.

33. **Cárdenas-Guerra RE, Arroyo R, Rosa de Andrade I, Benchimol M, Ortega-López J.** 2013. The iron-induced cysteine proteinase TvCP4 plays a key role in *Trichomonas vaginalis* haemolysis. Microbes Infect **15**:959–968.

34. **ter Kuile BH.** 1996. Metabolic adaptation of *Trichomonas vaginalis* to growth rate and glucose availability. Microbiology **142**:3337–3345. http://dx.doi.org/10.1099/13500392-142-12-3337.

35. **Carlton JM, Hirt RP, Silva JC, Delcher AL, Schatz M, Zhao Q, Wortman JR, Bidwell SL, Alsmark UCM, Besteiro S, Sicheritz-Ponten T, Noel CJ, Dacks JB, Foster PG, Simillion C, Van de Peer Y, Miranda-Saavedra D, Barton GJ, Westrop GD, Müller S, Dessi D, Fiori PL, Ren Q, Paulsen I, Zhang H, Bastida-Corcuera FD, Simoes-Barbosa A, Brown MT, Hayes RD, Mukherjee M, Okumura CY, Schneider R, Smith AJ, Vanacova S, Villalvazo M, Haas BJ, Pertea M, Feldblyum TV, Utterback TR, Shu CL, Osoegawa K, de Jong PJ, Hrdy I, Horvathova L, Zubacova Z, Dolezal P, Malik SB, Logsdon JM, Jr, Henze K, Gupta A, Wang CC, Dunne RL, Upcroft JA, Upcroft P, White O, Salzberg SL, Tang P, Chiu CH, Lee YS, Embley TM, Coombs GH, Mottram JC, Tachezy J, Fraser-Liggett CM, Johnson PJ.** 2007. Draft genome sequence of the sexually transmitted pathogen *Trichomonas vaginalis*. Science **315**:207–212. http://dx.doi.org/10.1126/science.1132894.

36. **Li WH, Yang J, Gu X.** 2005. Expression divergence between duplicate genes. Trends Genet **21**:602–607. http://dx.doi.org/10.1016/j.tig.2005.08.006.

37. **Qian W, Zhang J.** 2009. Protein subcellular relocalization in the evolution of yeast singleton and duplicate genes. Genome Biol Evol **1**:198–204. http://dx.doi.org/10.1093/gbe/evp021.

38. **Marcos CM, de Oliveira HC, da Silva JF, Assato PA, Fusco-Almeida AM, Mendes-Giannini MJ.** 2014. The multifaceted roles of metabolic enzymes in the *Paracoccidioides* species complex. Front Microbiol **5**:719–730. http://dx.doi.org/10.3389/fmicb.2014.00719.

39. **Jeffery CJ.** 2016. Protein species and moonlighting proteins: very small changes in a protein's covalent structure can change its biochemical function. J Proteomics **134**:19–24. http://dx.doi.org/10.1016/j.jprot.2015.10.003.

40. **Hirt RP, de Miguel N, Nakjang S, Dessi D, Liu YK, Diaz N, Rappelli P, Acosta-Serrano A, Fiori PL, Mottram J.** 2011. *Trichomonas vaginalis* pathobiology: new insights from the genome sequence. Adv Parasitol **77**:87–140. http://dx.doi.org/10.1016/B978-0-12-391429-3.00006-X.

41. **Hirt RP, Noel CJ, Sicheritz-Ponten T, Tachezy J, Fiori PL.** 2007. *Trichomonas vaginalis* surface proteins: a view from the genome. Trends Parasitol **23**:540–547. http://dx.doi.org/10.1016/j.pt.2007.08.020.

42. **Gould SB, Woehle C, Kusdian G, Landan G, Tachezy J, Zimorski V, Martin WF.** 2013. Deep sequencing of *Trichomonas vaginalis* during the early infection of vaginal epithelial cells and amoeboid transition. Int J Parasitol **43**:707–719. http://dx.doi.org/10.1016/j.ijpara.2013.04.002.

43. **Papp B, Pál C, Hurst LD.** 2003. Evolution of cis-regulatory elements in duplicated genes of yeast. Trends Genet **19**:417–422. http://dx.doi.org/10.1016/S0168-9525(03)00174-4.

44. **Lara-Gonzalez S, Estrella P, Portillo C, Cruces ME, Jimenez-Sandoval P, Fattori J, Migliorini-Figueira AC, Lopez-Hidalgo M, Diaz-Quezada C, Lopez-Castillo M, Trasviña-Arenas CH, Sanchez-Sandoval E, Gómez-Puyou A, Ortega-Lopez J, Arroyo R, Benítez-Cardoza CG, Brieba LG.** 2015. Substrate-induced dimerization of engineered monomeric variants of triosephosphate isomerase from *Trichomonas vaginalis*. PLoS One **10**:e0141747. http://dx.doi.org/10.1371/journal.pone.0141747.

45. **Twu O, de Miguel N, Lusting G, Stevens GC, Vashisht AA, Wohlschlegel JA, Johnson PJ.** 2013. *Trichomonas vaginalis* exosomes deliver cargo to host cell and mediate host:parasite interactions. PLoS Pathog **9**:e1003482. http://dx.doi.org/10.1371/journal.ppat.1003482.

46. **Ding Y, Wang J, Wang J, Stierhof YD, Robinson DG, Jiang L.** 2012. Unconventional protein secretion. Trends Plant Sc **17**:606–615. http://dx.doi.org/10.1016/j.tplants.2012.06.004.

47. **Potrykus J, Mahaney B, White RL, Bearne SL.** 2007. Proteomic investigations of glucose metabolism in the butyrate-producing gut anaerobe *Fusobacterium varium*. Proteomics **7**:1839–1853. http://dx.doi.org/10.1002/pmic.200600464.

48. **Crouch ML, Alderete JF.** 1999. *Trichomonas vaginalis* interactions with fibronectin and laminin. Microbiology **145**:2835–2843. http://dx.doi.org/10.1099/00221287-145-10-2835.

49. **Biller L, Matthiesen J, Kühne V, Lotter H, Handal G, Nozaki T, Saito-Nakano Y, Schümann M, Roeder T, Tannich E, Krause E, Bruchhaus I.** 2014. The cell surface proteome of *Entamoeba histolytica*. Mol Cell Proteomics **13**:132–144. http://dx.doi.org/10.1074/mcp.M113.031393.

50. **Serrano-Fujarte I, López-Romero E, Cuéllar-Cruz M.** 2016. Moonlight-like proteins of the cell wall protect sessile cells of *Candida* from oxidative stress. Microb Pathog **90**:22–33. http://dx.doi.org/10.1016/j.micpath.2015.10.001.

51. **Lal K, Noel CJ, Field MC, Goulding D, Hirt R.** 2006. Dramatic reorganization of *Trichomonas* endomembranes during amoebal transformation: a possible role of G-proteins. Mol Biochem Parasitol **148**:99–102. http://dx.doi.org/10.1016/j.molbiopara.2006.02.022.

52. **Gómez-Arreaza A, Acosta H, Quiñones W, Concepción JL, Michels PA, Avilán L.** 2014. Extracellular functions of glycolytic enzymes of parasites: unpredicted use of ancient proteins. Mol Biochem Parasitol **193**:75–81. http://dx.doi.org/10.1016/j.molbiopara.2014.02.005.

53. **Collingridge PW, Brown RWB, Ginger ML.** 2010. Moonlighting enzymes in parasitic protozoa. Parasitol **137**:1467–1475. http://dx.doi.org/10.1017/S0031182010000259.

54. **Varland S, Osberg C, Arnesen T.** 2015. N-terminal modifications of cellular proteins: the enzymes involved their substrate specificities and biological effects. Proteomics **15**:2385–2401. http://dx.doi.org/10.1002/pmic.201400619.

55. **Aicart-Ramos C, Valero RA, Rodriguez-Crespo I.** 2011. Protein palmitoylation and subcellular trafficking. Biochim Biophys Acta **1808**:2981–2994. http://dx.doi.org/10.1016/j.bbamem.2011.07.009.

56. **Linder ME, Deschenes RJ.** 2007. Palmitoylation: policing protein stability and traffic. Nat Rev Mol Cell Biol **8**:74–84. http://dx.doi.org/10.1038/nrm2084.

57. **Ramiah K, van Reenen CA, Dicks LM.** 2008. Surface-bound proteins of *Lactobacillus plantarum* 423 that contribute to adhesion of Caco-2 cells and their role in competitive exclusion and displacement of *Clostridium sporogenes* and *Enterococcus faecalis*. Res Microbiol **159**:470–475. http://dx.doi.org/10.1016/j.resmic.2008.06.002.

58. **Bao S, Chen D, Yu S, Chen H, Tan L, Hu M, Qiu X, Ding C.** 2015. Characterization of triosephosphate isomerase from *Mycoplasma gallisepticum*. FEMS Microbiol Lett **362**:fnv140. http://dx.doi.org/10.1093/femsle/fnv140.

59. **De Miguel M, Lustig G, Twu O, Chattopadhyay A, Wohlschlegel JA, Johnson PJ.** 2010. Proteome analysis of the surface of *Trichomonas vaginalis* reveals novel proteins and strain-dependent differential expression. Mol Cell Proteomics **9**:1554–1566. http://dx.doi.org/10.1074/mcp.M000022-MCP201.

60. **Ehrström S, Yu A, Rylander E.** 2006. Glucose in vaginal secretions before and after oral glucose tolerance testing in women with and without recurrent vulvovaginal candidiasis. Obstet Gynecol **108**:1432–1437. http://dx.doi.org/10.1097/01.AOG.0000246800.38892.fc.

61. **Goswami R, Dadhwal V, Tejaswi S, Datta K, Paul A, Haricharan RN, Banerjee U, Kochupillai NP.** 2000. Species-specific prevalence of vaginal candidiasis among patients with diabetes mellitus and its relation to their glycaemic status. J Infect **41**:162–166. http://dx.doi.org/10.1053/jinf.2000.0723.

62. **Goswami D, Goswami R, Banerjee U, Dadhwal V, Miglani S, Lattif AA, Kochupillai N.** 2006. Pattern of *Candida* species isolated from patients with diabetes mellitus and vulvovaginal candidiasis and their response to single dose oral fluconazole therapy. J Infect **52**:111–117. http://dx.doi.org/10.1016/j.jinf.2005.03.005.